TRANSPORT CHARACTERISTICS OF AMORPHOUS SEMICONDUCTORS IN THE DILUTE CARRIER REGIME: A VARIABLE RANGE HOPPING TREATMENT

A THESIS IN
Physics

Presented to the Faculty of the University
of Missouri-Kansas City in partial fulfillment of
the requirements for the degree

MASTER OF SCIENCE

by
NASEER ABDULHAMID DARI

B.S. Physics, University of Missouri-Kansas City, 2008
Kansas City, Missouri

Kansas City, Missouri
2010

TRANSPORT CHARACTERISTICS OF AMORPHOUS SEMICONDUCTORS IN THE DILUTE CARRIER REGIME: A VARIABLE RANGE HOPPING TREATMENT

Naseer Abdulhamid Dari, Candidate for the Master of Science Degree

University of Missouri-Kansas City

ABSTRACT

We survey the analytical methods which are used to find the conductivity of amorphous solids as a function of temperature, specifically the work done by N. F. Mott and Apsley et al. and we point out the problems with deriving such a relationship. We then develop a self consistent numerical system for calculating the charge occupancy factors, and apply it to a specific case of amorphous boron carbide, where positional disorder is introduced by incorporating random shifts in the positions and orientations of icosahedral clusters of boron and carbon atoms in an initially pristine rhombohedral arrangement of icosahedra. We find the transport characteristics to be most sensitive to the size of the icosahedral clusters relative to their mean separation, while it is robust with respect to disorder. In particular, the transport characteristics are only mildly affected (i.e. slightly diminished) by random displacements in the icosahedral positions, while they do not appear to be discernibly changed in the presence of even significant orientational disorder.

APPROVAL PAGE

The faculty listed below, appointed by the Dean of the College of Arts and Sciences, have examined a thesis titled, “Transport Characteristics of Amorphous Semiconductors in the Dilute Carrier Regime: A Variable Range Hopping Treatment”, presented by Naseer Abdulhamid Dari, candidate for the Master of Science degree, and certify that in their opinion it is worthy of acceptance.

Supervisory Committee

Donald Priour, Ph.D., Committee Chair
Department of Physics

Anthony Caruso, Ph.D.
Department of Physics

Da-Ming Zhu, Ph.D.
Department of Physics

CONTENTS

LIST OF ILLUSTRATIONS

CHAPTER 1

OVERVIEW

Introduction

The physical properties of amorphous materials have been a subject that is rarely treated in solid state physics. The lack of long range structure in this class of materials is a large barrier to developing an analytical model which describes their behavior adequately. One of the most frequently studied physical properties of amorphous solids is their electrical carrier conduction behavior, specifically at low temperature ranges. Here, we shall review some of the more important works to arrive at an analytical relationship describing the conduction in amorphous solids as a function of Temperature. We will further show why such endeavors may not be fruitful, due to the character of the assumptions required to arrive at an analytical relationship, and due to the careless application of these relationships without careful consideration of the geometrical systems to which they are applied. Moreover we shall show how this analytical relationship leads to unreasonable results, even when they appear to match the experimental measured conductivity without such considerations. We then review an alternative method to solve this problem, and attempt to refine its methodology by applying the approach to a situation with strong disorder.

In highly disordered amorphous materials, the wave functions of the various states within the system do not usually overlap. However, it is important to note here that due to the random nature of this system, it is possible that a few isolated clusters of

states where wave functions do overlap may appear in rare instances; however, such localized and isolated clusters do not alter the general behavior of the system when compared to the case where they do not arise. As such, we will consider a system where the states have a highly localized hydrogen-like wave function. In such a system, the conductivity will vanish at zero temperature due to the inexistence of extended states as they will allow non-zero conductivity at zero Kelvin due to not requiring thermal activation energy.

Mott's Model of Conductivity in Amorphous Materials

One of the most widely known and applied models of conductivity in amorphous materials is one advanced by N.F. Mott [1]. In his original paper, Mott proposed that the conductivity in amorphous materials is proportional to the inverse of the fourth root of the temperature, in the low temperature regime for materials with high degree of disorder and localized states. The analytical relationship has been the topic of debate, and over the years the theoretical foundation of Mott's derivation has been challenged and many attempts have been made to re-drive it more systematically. Some success has been made in this front. The mathematically elegant treatment of N. Apsley and P. Huges [2] has been among the most successful, as it avoids a particularly drastic assumption in Motts analysis: that the hopping energy is related inversely to the cube of distance hopped. Here we will have an overview of the theory developed by Mott to describe the conduction in doped semi-conductors vis a vis the refinements made by Apsley et al. and others.

Conductivity in amorphous solids at lower temperatures follows a form which is closely related to impurity conduction in doped and compensated semiconductors [1]. If our sites are highly localized, then the conduction occurs in an energy range between the valance band and conduction band. Let's assume that there are N donor levels per unit volume in the region between the aforementioned bands. If no acceptors are present, then conduction only occurs when an electron is thermally excited into the conduction band. However if cN acceptors are present (with c <1), then a proportion c of the donors will lose their electrons to an acceptor; therefore electrons can tunnel between various occupied donors to empty ones (see Fig. 1).

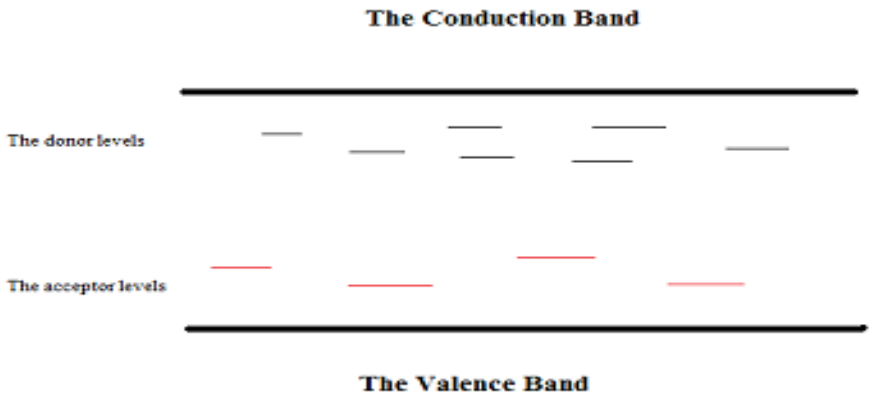

Figure 1. A schematic rendition of the hopping region in semi-conductors

At liquid helium temperature this is the dominant conduction mechanism, which requires some activation energy as pointed out by Miller and Abrahams [3]. The activation energy is generated from the thermal fluctuation within the structure of the

amorphous material. As such, as the temperature raises, the "thermally assisted hopping" form of conductivity increases, up to a certain limit (usually around room temperature) where this conductivity regime ceases, and gives way to other forms of conductivity such as trap-limited transport via intermittent excitation and to motion within extended states. The thermally assisted hopping process is in large measure mediated by the excitation of phonon modes (i.e. quantized lattice vibrations), which facilitate the charge transfer. Since a detailed treatment of the phonons is materials specific and in principle rather complicated, we follow the custom in variable range hopping theoretical calculations, and operate in a generalized framework which does not address the hopping mechanism in a precise way.

The fundamental model we examine is a picture in which transport is mediated by hops from occupied to unoccupied sites where the probability of a jump to occur between two sites with the spatial separation r and energy separation w is assumed to have the form:

$$P \sim exp[-2\alpha r - \frac{w}{kT}]$$

Where α^{-1} is the attenuation length for a hydrogen-like localized wave-function, as consistent with our assumptions above. Now we can introduce the reduced variables

$$r' = 2\alpha r, \quad w' = w/kT$$

so that

$$P \sim \exp[-r' - w'].$$

Since in a highly amorphous material, the energy and the spatial locations of sites are taken to be completely uncorrelated, the spatial and the energy components of the probability (*r'* and *w'* respectively) can be combined into a single variable, the Range, denoted as *R*. therefore

$$P \sim \exp[-R]$$

Here *R* represents the "location" of each site in the four dimensional space with three spatial coordinates and a single energy coordinate. The probability of success of a hopping attempt between two sites is therefore completely fixed by this range parameter, with the probability of a jump increasing monotonically with the decreasing range *R*. Conduction at a macroscopic scale is a result of many such hops, and as shorter hops are favored, the average nearest neighbor "distance" between the sites has a significant influence on the conductivity of the doped semi-conductor.

On a heuristic basis, one might expect

$$\sigma \sim exp\ [-R_{nn}]$$

or

$$ln(\sigma) = D(-R_{nn})$$

Here R_{nn} is the "average nearest neighbor range" and *D* is a constant. In Mott's theory, the task of calculating the conduction is assumed to be reduced to the calculation of this quantity. In subsequent discussion we point out the serious flaws in making this assumption, however for now let us precede with the usual method with which this quantity is calculated analytically following Mott's prescription.

The first task is to calculate *N(R)*, the total number of states with the range *R* of some initial state at the Fermi level. This can be calculated by carrying out the integral:

$$N(R) = \frac{N\pi kT}{2\alpha^3} \iint dr'dw' r'^2$$

in the reduced coordinates. The low boundary for the energy difference between the sites is of course zero, and the maximum cannot be greater than the bandwidth gap between the valence and the conduction bands. The spatial integration is constrained between the minimum of *2αa* where *a* is the nearest neighbor atomic spacing, and *r'*, the spatial part of the range we consider.

We now define the number of states with ranges between R and *R+dR* to be *ΔN(R) dR* where

$$\Delta N(R) = {}^{\delta N(R)}/_{\delta R}.$$

Then the probability that a state with range *R* is the nearest neighbor in this four dimensional space is:

$$P_{nn}(R) = \Delta N(R)\exp[-N(R)].$$

From this point on, these relationships can be applied to specific cases of interest, as was done by Apsley et al [2]. In that work, the treatment yields Mott's relationship:

$$\ln(\sigma) \sim A - BT^{1/4}$$

without resorting to his simplifying (though fairly drastic) assumption

The Problems Associated with Mott's Relationship

Over the years, further attempts have been made to refine the derivation; however a few problems persist. The majority of the problems with the analysis done by Mott has been pointed out in the work by J. M. Marshall and C. Main [4], and can be grouped in two categories: analytical problems and experimental discrepancies.

Analytical Problems of Mott's Treatment

The analytical problems with Mott's relationship lie in the very large number of assumptions necessary to simplify the physical situation into one which can be handled with a simple analytical treatment. Further, even with the simplified model, many anomalies arise, mainly due to the fact that Mott used a parameter, r_{max} , to denote the average hopping distance, and the radius of the sphere within which hopping occurs [4].

Although an effort was made by Mott to address this issue in [5], the revised analysis is however still incomplete; for instance it fails to account for the hops over various distances within the sphere [4].

Another significant issue with the analytical solution is the consideration of the nearest neighbor hopping, whereas variable range hopping in principle occurs in a more extended scheme in which site more distant than merely the nearest neighbor may be accessed. It was shown in [6] that the consideration of only the nearest neighbor leads to inaccuracies when a computational method was attempted for the iso-energetic case. As the number of the nearest neighbors was increased, the accuracy of the generated data improved, due to the reduction in the frequency of incidence of a spurious phenomenon described as the "trapping of the electron". For instance, if an electron jumps into a site which has a mutual nearest neighbor relationship with another, then the electron will

continuously jump between these two sites, and become essentially trapped, never straying beyond the two neighboring sites. The occurrence of this situation was estimated to be around 30 to 35% of the cases. While increasing the number of nearest neighbors does not fully eliminate this phenomenon, higher numbers reduce its possibility at an exponential rate. It was shown that the trapping happens at around about once in each 10,000 attempts when the nearest neighbor count reaches 8, which generates results that are very close to the experimental values. We argue that a theoretical model which describes conductivity must hold in iso-energetic cases and in cases where the energy of the sites differs. Therefore we believe that this is a further indication of the shortcoming of Mott's analytical treatment as in all derivations either explicitly use the nearest neighbor, or implicitly lose all other neighbors in the averaging mechanisms which they employ.

Experimental Discrepancies

Significant discrepancies with empirical data can be readily seen in many experiments where the predicted conductivity is off by up to 20 orders of magnitude [4]. Moreover, in cases, where the predicted conductivity matches the experimental one, a more detailed analysis of the model leads to unreasonable density of states (DOS). For example in [7], values of DOS were calculated to be between 10^{25} and 10^{28} cm^{-3} eV^{-1} for their various specimens of RF sputtered amorphous Group IV materials. The DOS is not expected to exceed 10^{21} cm^{-3} eV^{-1} as metallic conduction becomes the dominant form of conduction in regimes where the DOS is higher.

It is important to note here that we are not suggesting that the Mott's treatment is wrong quantitatively. Rather we are suggesting that the issues with this model can be traced to its application without considering the general geometry of the amorphous material being studied. Further, some of the assumptions which turn out to be serious oversimplifications may be circumvented by using a computational method which we employ in our study of the transport characteristics of strongly disordered semiconductors.

A salient advantage of our method is the avoidance of many of the drastic assumptions which plagued Mott's treatment. All that is required here is that the Miller-Abrahams expression to be the rate of carriers jumps between the sites. Our computational method is heavily reliant on the underlying geometry of the case in study; specifically, we will examine randomly positioned Icosahedra with random "radii" which are set in a tetrahedral lattice with a tunable lattice constant. The procedure follows in Chapter 2.

CHAPTER 2
METHODOLOGY

Analytical Derivation

As noted above, in Apsley and Huges paper, the authors have used the average nearest neighbor range and used a heuristic argument about its relationship to the conductivity. In what follows present and examine the implications of a derivation in which this assumption is not made. As we have discussed before, the range is partially due to the spatial variations in three dimensions, and in part due to the variation in the energy. Therefore we believe that considering only the average of this quantity is in direct conflict with the strongly disordered nature of amorphous materials and hence inappropriate as a method to approach this issue.

It is important to note here that in the sections following the one dimensional case, we no longer attempt to derive the relationships analytically. Rather, we opt to arrive at the relationships which are pertinent to our implementation of the computer program.

One Dimensional System

We wish to first consider the iso-energetic, one dimensional case in the presence of an electric field, which will be fruitful in our later derivation. First let's assume that all sites have a uniform separation, given by r (see Fig. 2).

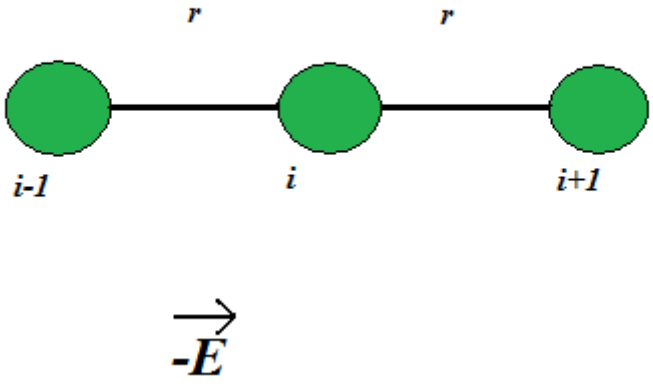

Figure 2. Iso-energetic, 1-D system in the presence of an electric field.

For this case, the probability of a jump from one site to another is given by

$$P \sim e^{-2\alpha r} g(w)$$

Where $w = ([\mathcal{E}\Delta r]e)$ and ε is the magnitude of the electric field and Δr is the special separation between the two sites. When $w > 0$ $g(w) = e^{-w/kT}$, and $g(w) = 1$ when $w < 0$. Thus jumps opposite to the direction of the electric field are favored and hence the net current goes in the opposite direction of the electric field. If we consider the case where the sites have uniform separation r, then the net current in the favorable direction to the nearest neighbor is:

$$I_{i,i+1} = e^{-2\alpha r}[f_i - f_{i+1}e^{-\frac{w}{kT}}]$$

Here the f_i denotes the term in which we've packaged the chemical potential at the site i, and is given by:

$$f_i = e^{\frac{\mu_i}{kT}}$$

In the simplest case which we examine here, the f-factors of all sites is the same, thus we can write:

$$I_{i,i+1} = f_i e^{-2\alpha r}\left[1 - e^{-\frac{w}{kT}}\right]$$

We now want to examine the total current leaving a site to all other sites in the favorable direction. To do this, we must sum over all possible sites in that direction, so we have:

$$I_{i,j} = f_i \sum_{j=1}^{\infty} e^{-2\alpha j r}\left(1 - e^{-j\frac{w}{kT}}\right)$$

Denoting as $A=2\alpha r$, and noting that $w \ll kT$ we can write

$$I_{i,j} = f_i \sum_{j=1}^{\infty} e^{-2\alpha j r}\left(\frac{jw}{kT}\right)$$

Using the geometric series, we can find the general expression of the above as:

$$= f_i\left[\frac{e^{-A}}{1 - e^{-A}} - \frac{e^{-(A-w)}}{1 - e^{-(A-w)}}\right]$$

$$= f_i e^{-A}\left[\frac{1}{1 - e^{-A}} - \frac{e^{-w}}{1 - e^{-(A-w)}}\right]$$

$$= f_i e^{-A}\left[\frac{1}{1 - e^{-A}} - \frac{1 - w}{1 - (1 - w)e^{-A}}\right]$$

$$= f_i e^{-A}\left[\frac{1}{1 - e^{-A}} - \frac{1 - w}{(1 - e^{-A}) + we^{-A}}\right]$$

We shall only consider the terms which are no higher than first order in w, so now we have:

$$= f_i e^{-A}\left[\frac{1}{1-e^{-A}} - \frac{1}{(1-e^{-A})+we^{-A}} + \frac{w}{1-e^{-A}}\right]$$

And finally we have:

$$= \frac{f_i w e^{-A}}{(1-e^{-A})^2}$$

Now we can relax the condition that all sites have an equal separation by introducing a random perturbation to the location of each site, which will induce a shift the chemical potential at each site. The f-factor is then given by:

$$f_i = e^{\frac{\mu_o - \delta\mu_i}{kT}}$$

Where $\delta\mu_i$ represents the shift in the chemical potential in site *i*. As stated previously, we will now introduce a small perturbation to the location of each site, by letting it vary a small amount, given by η_i. The current in this case will be:

$$I_{i,i+1} = e^{-2\alpha r}\left[f_i e^{-2\alpha(\eta_{i+1}-\eta_i)} - f_{i+1}\left(1 - w(r+\eta_{i+1}-\eta_i)\right)e^{-2\alpha(\eta_{i+1}-\eta_i)}\right]$$

We can now work out the implications of charge conservation at each site, i.e.

$$\Phi_i^{in} = \Phi_i^{out}$$

Where Φ_i is the flux at site *i.* if we consider only the nearest neighboring sites to *i,* we can write:

$$\phi_i^{out} = f_i[e^{-2\alpha[r+\eta_{i+1}-\eta_i]} + e^{-2\alpha[r+\eta_{i-1}-\eta_i]}e^{(\frac{-w[r+\eta_i-\eta_{i-1}]}{kT})}]$$

And

$$\phi_i^{in} = f_{i-1}[e^{-2\alpha[r+\eta_i-\eta_{i-1}]}] + f_{i+1}[e^{-2\alpha[r+\eta_{i+1}-\eta_i]}e^{(\frac{-w[r+\eta_{i+1}-\eta_i]}{kT})}]$$

Equating the above two equations, and dividing out the $e^{-2\alpha r}$ we have:

$$f_i[e^{-\alpha[\eta_{i+1}-\eta_i]} + e^{-\alpha[\eta_{i-1}-\eta_i]}e^{(\frac{-w[r+\eta_i-\eta_{i-1}]}{kT})}] =$$

$$f_{i-1}[e^{-\alpha[\eta_i-\eta_{i-1}]}] + f_{i+1}[e^{-\alpha[\eta_{i+1}-\eta_i]}e^{(\frac{-w[r+\eta_{i+1}-\eta_i]}{kT})}]$$

As before, we may simplify this expression by noting $w \ll kT$, and substituting in the expression for f_i we have:

$$e^{\frac{\mu_o-\delta\mu_i}{kT}}[e^{-\alpha[\eta_{i+1}-\eta_i]} + e^{-\alpha[\eta_{i-1}-\eta_i]}\{1 - \frac{-w[r+\eta_i-\eta_{i-1}]}{kT}\}] =$$

$$e^{\frac{\mu_o-\delta\mu_{i-1}}{kT}}[e^{-\alpha[\eta_i-\eta_{i-1}]}] + e^{\frac{\mu_o-\delta\mu_{i+1}}{kT}}[e^{-\alpha[\eta_{i+1}-\eta_i]}\{1 - \frac{-w[r+\eta_{i+1}-\eta_i]}{kT}\}]$$

We may further simplify this by dividing both sides by $e^{\frac{\mu_o}{kT}}$, using the same assumption as the one dimensional case with no disorder, which was that all sites have the same chemical potential. The result would be:

$$e^{\delta\mu_i}[e^{-\alpha[\eta_{i+1}-\eta_i]} + e^{-\alpha[\eta_{i-1}-\eta_i]}\{1 - \frac{-w[r+\eta_i-\eta_{i-1}]}{kT}\}] =$$

$$e^{\delta\mu_{i-1}}[e^{-\alpha[\eta_i-\eta_{i-1}]}] + e^{\delta\mu_{i+1}}[e^{-\alpha[\eta_{i+1}-\eta_i]}\{1 - \frac{-w[r+\eta_{i+1}-\eta_i]}{kT}\}]$$

So now our task is to calculate the shifts in chemical potentials "$\delta\mu_i$", "$\delta\mu_{i+1}$", and "$\delta\mu_{i-1}$". However, it is more convenient to solve for the $e^{\frac{\delta\mu_i}{kT}}$ factors without seeking the shifts in chemical potentials directly.

To do this we shall make use of an iterative numerical method using a computer program which, given a good first choice, shall converge rapidly to the correct answer for the shift. An outline of the method follows.

From above we have:

$$e^{-\frac{\delta\mu_i}{kT}} = \frac{e^{\delta\mu_{i-1}}[e^{-\alpha[\eta_i-\eta_{i-1}]}] + e^{\delta\mu_{i+1}}[e^{-\alpha[\eta_{i+1}-\eta_i]}\{1-\frac{-w[r+\eta_{i+1}-\eta_i]}{kT}\}]}{[e^{-\alpha[\eta_{i+1}-\eta_i]} + e^{-\alpha[\eta_{i-1}-\eta_i]}\{1-\frac{-w[r+\eta_i-\eta_{i-1}]}{kT}\}]}$$

And we can use the notation $F_i^k = e^{\delta\mu_i^k}$ where the *"k"* superscript denotes the iteration number. So now we have:

$$F_i^{k+1} = \frac{F_{i-1}^k[e^{-\alpha[\eta_i-\eta_{i-1}]}] + F_{i+1}^k[e^{-\alpha[\eta_{i+1}-\eta_i]}\{1-\frac{-w[r+\eta_{i+1}-\eta_i]}{kT}\}]}{[e^{-\alpha[\eta_{i+1}-\eta_i]} + e^{-\alpha[\eta_{i-1}-\eta_i]}\{1-\frac{-w[r+\eta_i-\eta_{i-1}]}{kT}\}]}$$

Starting with an initial guess of $F_i^0 = 1$ we can successively get a closer and closer approximation to the $\delta\mu$. The spatial shifts, η_i, will be chosen from a normal distribution of width $\frac{r}{20}$, centered about zero. This perturbation width was chosen for two reasons: first a shift of one tenth of a lattice constant is the Lindemann Criterion [8] for the shift from a lattice to an amorphous system. The second reason is that even though we can allow a variation of up to one half of the lattice constant without disturbing the order of our lattice, the larger variations will introduce instability in our numerical methods. Thus we chose the range between - $\frac{r}{20}$ to $\frac{r}{20}$ to be the range in which we generated our random numbers.

Two Dimensional System: Triangular Lattice

We can approximate the icosahedrons to spheres. In a tight packing, these spheres will arrange themselves in such a way, that if we were to draw lines between the centers of each sphere, we would see that the lines form a tetrahedral lattice. It is therefore of interest to visit the two and three dimensional tetrahedral lattice structures.

Let us first look at the 2-D iso-energetic case, and at first, let's not introduce any positional disorder in the system (see fig. 3).

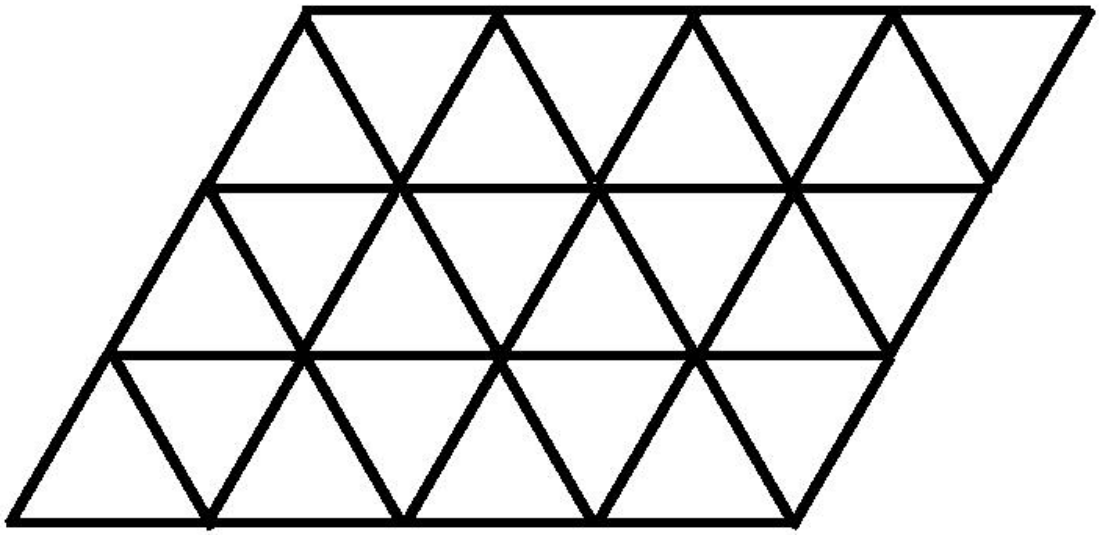

Figure 3. The 2-D Triangular Lattice.

Each site on the lattice has six nearest neighbors as well as six next nearest neighbors. The distance to the nearest neighbor is the lattice constant c, while the distance to the next nearest neighbor is $\sqrt{3}c$.

As before, we attempt to calculate the current in the 2-D iso-energetic, unperturbed lattice when subjected to an electric field within the context of variable range hopping. From the symmetry of the lattice we can immediately infer that $f_{i,j}$ factors are identical at every site in the triangular lattice. Also, the symmetry of the lattice will enforce charge conservation automatically. Now consider an electric field

oriented somewhere between 0 and $\frac{\pi}{3}$. Symmetry arguments tell us the magnitude of the current will show every possible angular variation within this $\frac{\pi}{3}$ interval and repeat as one continues to extend the angle beyond $\frac{\pi}{3}$ in the counterclockwise direction.

Let us examine the nearest neighbors, and see generally how to calculate the currents in the *x* and *y* directions.

$$\Phi_{i,j}^{i,j+1} = f_o e^{-\alpha c}[1 - e^{-w_x c}] \text{ where } w_x = \frac{E_x}{kT}$$

$$\approx f_o e^{-\alpha c} w_x c$$

Using the same method, one would be able to calculate the flux to each of the other nearest neighbors. However, we can make a much broader and more concise statement about the current fluxes. Consider the charge flux from a site labeled *k* to another labeled *k'*. The spatial hopping factor is simply $e^{-\alpha d_{kk'}}$ where $d_{kk'}$ denotes the distance separating the two points. The electrical energy term is $\boldsymbol{d}_{kk'} * \boldsymbol{E}$. if the shift in electric field is less than zero, then the electron is moving "downstream" and if it is greater than zero, then we are moving "upstream". We shall consider each possibility in turn.

If $\Delta E < 0$ then

$$\Phi_{k'}^{k} = f_o e^{-\alpha d}[1 - e^{\frac{-\Delta E}{kT}}] \approx f_o e^{-\alpha d} \frac{\Delta E}{kT}$$

Also if $\Delta E > 0$ then we also have:

$$\Phi_{k'}^{k} = f_o e^{-\alpha d}[e^{\frac{-\Delta E}{kT}} - 1] \approx f_o e^{-\alpha d} \frac{\Delta E}{kT}$$

Therefore we can see that, in general:

$$\Phi_{kl}^{k} \approx f_o e^{-\alpha d} \frac{\Delta E}{kT} = f_o e^{-\alpha d} (\boldsymbol{E}.\boldsymbol{d}_{kk'})$$

Now we can find the current associated with this flux as

$$\boldsymbol{I}_{kk'} = \frac{f_o e^{-\alpha d_{kk'}}}{kT} (\boldsymbol{E}.\boldsymbol{d}_{kk'}) \frac{\boldsymbol{d}_{kk'}}{d_{kk'}}$$

To find the total current we must sum over each of the accessible sites, so therefore we have:

$$\boldsymbol{I}_{k}^{total} = \sum_{k'} \frac{f_o e^{-\alpha d_{kk'}}}{kT} (\boldsymbol{E}.\boldsymbol{d}_{kk'}) \frac{\boldsymbol{d}_{kk'}}{d_{kk'}}$$

It is important to note here that this current is the current due to jumps to primary neighbors only. To find the full current one must add on the currents due to jump to the second and third nearest neighbors and so forth. We have done this, however, as the process and the results are very similar to the three dimensional case, we shall not review the two dimensional results here. Instead we shall visit the three dimensional case in greater detail.

As in the 1-D case, we now wish to introduce an element of disorder to the triangular 2-D lattice which will require a computer study. We introduce random shifts to the location of the sites in the triangular lattice which will result in changes to the charge factors f_{ij}. The machinery we develop here will be easy to generalize to more complicated lattices (e.g. the three dimensional FCC or tetrahedral lattice).

First let us calculate the current at each site assuming that the charge factors are known. In calculating the current, we must seek all neighbors within a specified range

which would typically be some multiple of the decay constant α^{-1}. The charge which will flow between two sites will be determined first

Consider the site *ij* and *i'j'*. The current will be in this case

$$I_{ij}^{i'j'} = Ae^{-\alpha d_{ij}^{i'j'}}$$

Where *A* is a factor which will depend on f_{ij}, $f_{i'j'}$ and the orientation and the strength of the electric field.

The key is to find the current relayed in each of the bonds, as we can then sum over these bonds for each site and divide by 2 to correct for the redundancies in the counting process. For example consider the bond connecting the sites *ij* and *i'j'*. Whether or not this move is "upstream" or "downstream" is an issue determined by the sign of the energy shift. We will examine both of these possibilities and obtain a corresponding result for the current in each case.

Recall that the energy shift between two sites is $([\boldsymbol{\mathcal{E}}.\boldsymbol{\Delta r}]e)$. First let's consider the downstream case where:

$$\boldsymbol{I}_{ij} = e^{-\alpha d_{ij}^{i'j'}}[f_{ij} - f_{i'j'}e^{\frac{-eEd_{ij}^{i'j'}}{kT}}]$$

$$= e^{-\alpha d_{ij}^{i'j'}}[f_{ij} - f_{i'j'} + f_{i'j'}\boldsymbol{W}\boldsymbol{d}_{\boldsymbol{ij}}^{\boldsymbol{i'j'}}]$$

where $= \frac{eE}{kT}$. The current $\boldsymbol{I}_{ij}^{i'j'}$ is directed along the line connecting *ij* to *i'j'* such that, for the downstream case we have:

$$I_{ij}^{i'j'} = e^{-\alpha d_{ij}^{i'j'}}[f_{ij} - f_{i'j'} + f_{i'j'}\boldsymbol{W}\boldsymbol{d}_{\boldsymbol{ij}}^{\boldsymbol{i'j'}}]\frac{d_{ij}^{i'j'}}{d_{ij}^{i'j'}}$$

With $\boldsymbol{w}.\boldsymbol{d}_{ij}^{i'j} > 0.$

For the upstream case, the situation differs as the travel from *ij* to *i'j'* will be suppressed by a thermal factor. For this case the work required for the movement of charge is positive. Then the expression for the current is:

$$\boldsymbol{I}_{ij} = e^{-\alpha d_{ij}^{i'j'}}\left[-f_{ij} + f_{i'j'}e^{\frac{eEd_{ij}^{i'j'}}{kT}}\right]$$

So then

$$I_{ij}^{i'j'} = e^{-\alpha d_{ij}^{i'j'}}\left[f_{ij} - f_{i'j'} + f_{i'j'}\boldsymbol{W}\boldsymbol{d}_{ij}^{i'j'}\right]\frac{d_{ij}^{i'j'}}{d_{ij}^{i'j'}}$$

Where $\boldsymbol{w}.\boldsymbol{d}_{ij}^{i'j} < 0.$

We have used the Miller-Abrahams prescription to obtain these formulas for the upstream and downstream cases. Now we wish to find a convenient way to refer to the current in both cases. For the present we will deal with each case separately and our analysis will bifurcate accordingly.

Let us next record an expression for the mean current flowing through the system. It will be natural in the two dimensional case to operate in the terms of the surface current density.

Our system is broken up into many sites with discrete link currents. We need to translate this into a macroscopic result by implementing an appropriate sum. Consider two very narrow slices through the system. In this example, if we wish to calculate the total current in the *x* direction, say, then the slices will have to be perpendicular to the x-axis. Due to charge conservation, the currents through each of these slices will be the

same or else the charge conservation is violated. We now wish to make these slices as narrow as possible to avoid encompassing any nodes within them. Moreover, if we include numerous (*N)* of these slices we will still obtain the same result due to current conservation principle, provided that we divide by the total number *N* of the slices.

So the current in the *x* direction will appear as:

$$\boldsymbol{I}_x^{total} = \sum_{i=1}^{N} \frac{slice_i}{N} = \sum_{i=1}^{N} \frac{slice_i \Delta x}{L}$$

where $\Delta x = \frac{L}{N}$ is the width of a slice. This expression will introduce a weighting which will depend on the length of each bond parallel to the x-axis. The larger the magnitude of the bond between two sites, the larger it's contribution to the current.

Thus, our sum giving the current in the *x*-direction may be summed over all the links, and it will have the form:

$$I_x = \frac{1}{2} \sum_{ij} \sum_{i'j'} (\boldsymbol{I}_{ij}^{i'j'} . \boldsymbol{x})(d_{ij}^{i'j'}) \frac{1}{L}$$

Similarly, the *y*-component is given by:

$$I_y = \frac{1}{2} \sum_{ij} \sum_{i'j'} \left(\boldsymbol{I}_{ij}^{i'j'} . \boldsymbol{y}\right)\left(d_{ij}^{i'j'}\right) \frac{1}{L}$$

And in this way, we may glean the currents with relative ease.

The current will depend on the f_{ij} factors for each site, and we need to calculate them. We will use a self-consistent procedure where we initially assume that the charge factors are identical up to a pre-factor f_o.

For each site, we will insist that the net charge flux is zero. In this manner we satisfy the condition for steady-state which prevents the accumulation of charge in the site. The flux outward will be proportional to the f_{ij} factor which we are trying to determine. In particular:

$$\Phi_{ij}^{out} = f_{ij} \sum_{x} \sum_{y} e^{-\alpha d_{ij}^{xy}} [\Theta_{ij}^{xy}]$$

Where *x* and *y* here denote the nearest neighbor along the respective direction, and the thermal factor Θ_{ij}^{xy} is as determined before, and it depends on whether one is moving up or downstream.

Let us now calculate the flux more explicitly, showing the distinct contributions for the upstream and downstream channels of charge transport. We have:

$$\Phi_{ij}^{out} = f_{ij}[\sum_{x_n^u} \sum_{y_n^u} e^{-\alpha d_{ij}^{x_n^u y_n^u}} e^{wd_{ij}^{x_n^u y_n^u}} + \sum_{x_n^D} \sum_{y_n^D} e^{-\alpha d_{ij}^{x_n^D y_n^D}}$$

Where the first set up summations is over the upstream neighbors, and the second set of summation is over the downstream neighbors. we may clean up the above expression by introducing a function, *G[x]* where *G[x]=1* when $x > 0$ and $G[x]=e^{-x}$ for $x < 0$. If we have $x << 1$, we may linearize and write $G[x] = 1-x$. using this formulation, and insisting on the steady-state condition of

$$\Phi_{ij}^{in} = \Phi_{ij}^{out}$$

We can solve for f_{ij} using an iterative scheme similar to the one dimensional case as:

$$f_{ij}^{N+1} = \frac{\sum_{xn}\sum_{yn} f_{xn,yn}^{N} e^{-\alpha d_{ij}^{xn,yn}} G[-\boldsymbol{W}.\boldsymbol{d}_{ij}^{x_n y_n}]}{\sum_{xn}\sum_{yn} e^{-\alpha d_{ij}^{xn,yn}} G[\boldsymbol{W}.\boldsymbol{d}_{ij}^{x_n y_n}]}$$

The currents and other quantities needed may be calculated after a suitable level of convergence has been achieved. To check for such condition we will calculate a residual quantity that would vanish in the event of convergence. This residual term which will use is:

$$p = \frac{1}{N_s^2}\frac{|\Phi_{in} - \Phi_{out}|}{|\Phi_{in} + \Phi_{out}|}$$

Here N_s is the total number of sites in the system. For the purposes of our calculation, we will insist that the residual term P has fallen below one part in 10^5 in order to conclude that convergence has been accomplished. The calculations in the FORTRAN code shall continue until $P < 10^{-5}$.

One final task remains before we can fully implement this program: the identification of the vector $\boldsymbol{d}_{ij}^{i'j'}$ which connects the sites *ij* and *i'j'*. As mentioned previously, the idea is to introduce small perturbations in the *x* and *y* locations of the sites on the triangular lattice. Our aim is to see what happens to the current as we disrupt the lattice, and we will examine the effects of changing the magnitude of the perturbations and while considering different values of α, the length scale of the decay of the wave function overlap. In this scheme which we consider, the perturbed coordinates for the sites in the two dimensional triangular lattice will be

$$X_{ij} = i + \frac{j}{2} + \eta_{ij}^{x}$$

$$Y_{ij} = \frac{\sqrt{3}}{2} j + \eta_{ij}^{y}$$

With this information we are able to determine the distance between two sites, where the distance would have the form:

$$d_{ij}^{i'j'} = \sqrt{([i'-j] + \frac{1}{2}[j'-i] + \eta_{i'j'}^{x} - \eta_{ij}^{x})^2 + (\frac{\sqrt{3}}{2}[j'-i] + \eta_{i'j'}^{y} - \eta_{i'j'}^{y})^2}$$

Systems with Three Dimensions: The Tetrahedral Lattice

Again, for this case we use the general formula:

$$\boldsymbol{I}_{k}^{total} = \sum_{k'} \frac{f_o e^{-\alpha d_{kk'}}}{kT} (\boldsymbol{E}.\boldsymbol{d}_{kk'}) \frac{\boldsymbol{d}_{kk'}}{d_{kk'}} = \boldsymbol{I}^{primary} + \boldsymbol{I}^{secondary} + \boldsymbol{I}^{tertiary}$$

Let us now calculate the contribution of the primary, secondary, and tertiary currents to the total current. We note here that $\boldsymbol{E} = [E_x + E_y + E_z]$. For the vector displacements corresponding to the sites in the Cartesian Coordinates we shall use:

$$\boldsymbol{V} = [\Delta i + \frac{1}{2}(\Delta j + \Delta k), \frac{\sqrt{3}}{2}\Delta j + \frac{1}{2\sqrt{3}}\Delta k, \sqrt{\frac{2}{3}}\Delta k]$$

Using the above equation we can systematically write the position of the 12 primary nearest neighbors to a site *[i,j,k]* by only considering the vector shifts associated with the new site as shown below:

$$(1,0,0):\ \boldsymbol{V}_1^1 = c[1,0,0]\ ;\ (-1,0,0):\ \boldsymbol{V}_2^1 = -c[1,0,0]$$

$$(0,1,0):\ \boldsymbol{V}_3^1 = c\left[\frac{1}{2}, \frac{\sqrt{3}}{2}, 0\right]\ ;\ (0,-1,0):\ \boldsymbol{V}_4^1 = -c\left[\frac{1}{2}, \frac{\sqrt{3}}{2}, 0\right]$$

$$(0,0,1):\ \boldsymbol{V}_5^1 = c\left[\frac{1}{2},\frac{1}{2\sqrt{3}},\sqrt{\frac{2}{3}}\right]\ ;\ \ (0,0,-1):\ \boldsymbol{V}_6^1 = -c\left[\frac{1}{2},\frac{1}{2\sqrt{3}},\sqrt{\frac{2}{3}}\right]$$

$$(1,-1,0):\ \boldsymbol{V}_7^1 = c\left[\frac{1}{2},\frac{-\sqrt{3}}{2},0\right]\ ;\ \ (-1,1,0):\ \boldsymbol{V}_8^1 = -c\left[\frac{1}{2},\frac{-\sqrt{3}}{2},0\right]$$

$$(1,0,-1):\ \boldsymbol{V}_9^1 = c\left[\frac{1}{2},\frac{-1}{2\sqrt{3}},-\sqrt{\frac{2}{3}}\right]\ ;\ \ (-1,0,1):\ \boldsymbol{V}_{10}^1 = -c\left[\frac{1}{2},\frac{-1}{2\sqrt{3}},-\sqrt{\frac{2}{3}}\right]$$

$$(0,1,-1):\ \boldsymbol{V}_{11}^1 = c\left[0,\frac{1}{\sqrt{3}},-\sqrt{\frac{2}{3}}\right]\ ;\ \ (0,-1,1):\ \boldsymbol{V}_{12}^1 = -c\left[0,\frac{1}{\sqrt{3}},-\sqrt{\frac{2}{3}}\right]$$

Now, armed with these vectors (each of length *a*) we may write the current due to the jumps to the primary neighbors as:

$$\boldsymbol{I}_{ijk}^1 =$$

$$\frac{f_o e^{-\alpha a}}{kT} c[E_x(1,0,0) - E_x(1,0,0) + \left(\frac{E_x}{2} + \frac{\sqrt{3}E_y}{2}\right)\left(\frac{1}{2},\frac{\sqrt{3}}{2},0\right) +$$

$$\left(-\frac{E_x}{2} - \frac{\sqrt{3}E_y}{2}\right)\left(-\frac{1}{2},-\frac{\sqrt{3}}{2},0\right) + \left(\frac{E_x}{2} + \frac{E_y}{2\sqrt{3}} + \sqrt{\frac{2}{3}}E_z\right)\left(\frac{1}{2},\frac{1}{2\sqrt{3}},\sqrt{\frac{2}{3}}\right) + \left(-\frac{E_x}{2} - \frac{E_y}{2\sqrt{3}} -$$

$$\sqrt{\frac{2}{3}}E_z\right)\left(-\frac{1}{2},-\frac{1}{2\sqrt{3}},-\sqrt{\frac{2}{3}}\right) + \left(\frac{E_x}{2} - \frac{\sqrt{3}E_y}{2}\right)\left(\frac{1}{2},-\frac{\sqrt{3}}{2},0\right) + \left(-\frac{E_x}{2} + \frac{\sqrt{3}E_y}{2}\right)\left(-\frac{1}{2},+\frac{\sqrt{3}}{2},0\right) +$$

$$(\frac{E_x}{2} - \frac{E_y}{2\sqrt{3}} - \sqrt{\frac{2}{3}}E_z)(\frac{1}{2},-\frac{1}{2\sqrt{3}},-\sqrt{\frac{2}{3}}) + \left(-\frac{E_x}{2} + \frac{E_y}{2\sqrt{3}} + \sqrt{\frac{2}{3}}E_z\right)\left(-\frac{1}{2},+\frac{1}{2\sqrt{3}},+\sqrt{\frac{2}{3}}\right) +$$

$$\left(\frac{E_y}{\sqrt{3}} - \sqrt{\frac{2}{3}}E_z\right)\left(0,\frac{1}{\sqrt{3}},-\sqrt{\frac{2}{3}}\right) + \left(-\frac{E_y}{\sqrt{3}} + \sqrt{\frac{2}{3}}E_z\right)(0,-\frac{1}{\sqrt{3}},+\sqrt{\frac{2}{3}})]$$

This after some algebra finally simplifies to:

$$\boldsymbol{I}_{ijk}^{1} = \frac{f_o e^{-\alpha c}}{kT}(4c)[E_x, E_y, E_z]$$

To find the current flow to the secondary nearest neighbors, we find that in the 3-D case we have six such neighbors, each separated from our site of interest by a distance $\sqrt{2}c$. Using the same methodology as above, we can find the vector shifts corresponding to each site, and then calculate the net current flow to these sites. Our calculations show that this current is given by:

$$\boldsymbol{I}_{ijk}^{2} = \frac{f_o c\sqrt{2}}{kT} e^{-\sqrt{2}\alpha c}\left[\left(3E_x - \frac{-E_y}{\sqrt{3}} + \sqrt{\frac{2}{3}}E_z\right), \left(E_y - \frac{E_x}{\sqrt{3}} - \sqrt{2}E_z\right), \left(2E_z - \sqrt{2}E_y + \sqrt{\frac{2}{3}}E_x\right)\right]$$

The next step would be to find the current produced from jumps to the 18 tertiary nearest neighbors. As the reader can see, this is a very complex task. We have carrier this task, and believe no additional information can be seen from writing the process here. It is sufficient to note that the complexity of the task lends itself very well to being handled numerically using a computing device, which is what we have done. There is one final step to our calculation. We now wish to replace each site on the tetrahedral 3-D lattice by an icosahedron, at which point we may introduce random perturbation about the distances between the icosahedra, and also randomly produce deformity in the icosahedra themselves by removing vertices randomly. It is pertinent here to have a review of the geometry of icosahedrons.

Icosahedral Geometry

In some respects our initial treatment will be an idealization. On the other hand, we will also endeavor to give a rigorous treatment to the geometry of Icosahedrons.

An icosahedron stands among platonic solids in that all sides and faces are identical, or congruent. Icosahedrons have 12 vertices, 30 edges, and 20 triangular faces. A perspective of "exploded" icosahedral geometry is given in fig. 4, which shall be hereafter our method of cataloging the vertices and helps to further illustrate the geometrical relationships among the vertices.

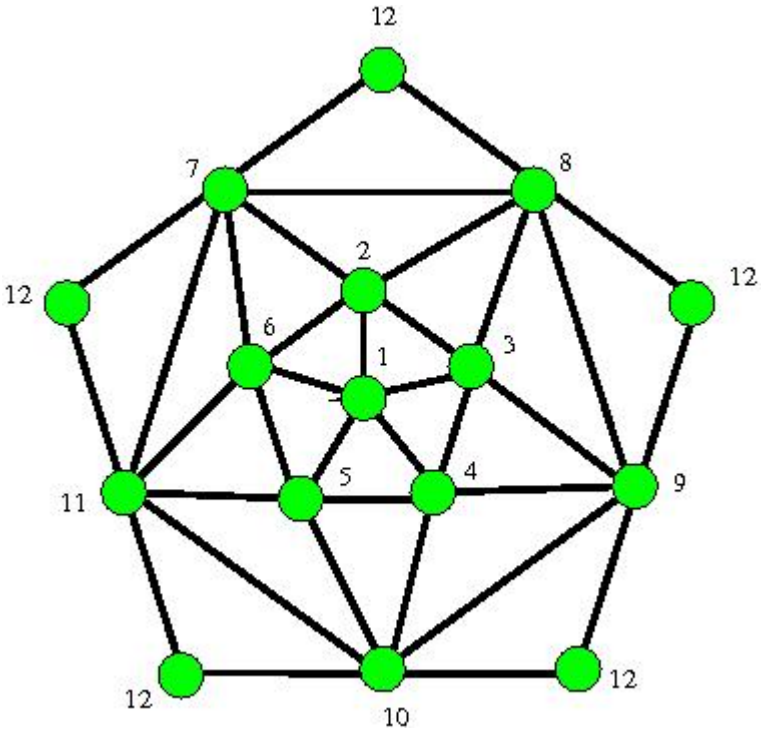

Figure 4. The "Exploded" Icosahedron with the labeled vertices

It will be convenient to operate in the spherical coordinates, where each vertex sits on the surface of a circumscribing sphere of radius *R.* as such, when we refer to the "radius" of the icosahedrons, we are referring to the radius of this sphere. Among other things, we would like to calculate *R* in terms of the edge length *S*. in addition, we would like to identify each of the 12 vertices in spherical coordinates. If we operate in this manner it would be easier to perform rotations of the icosahedral shells. We will separately address the points on the upper hemisphere and those on the lower hemisphere.

The upper vertices include the absolute apex, given by label 1, and the surrounding five points in a pentagonal arrangement as illustrated below in fig. 5.

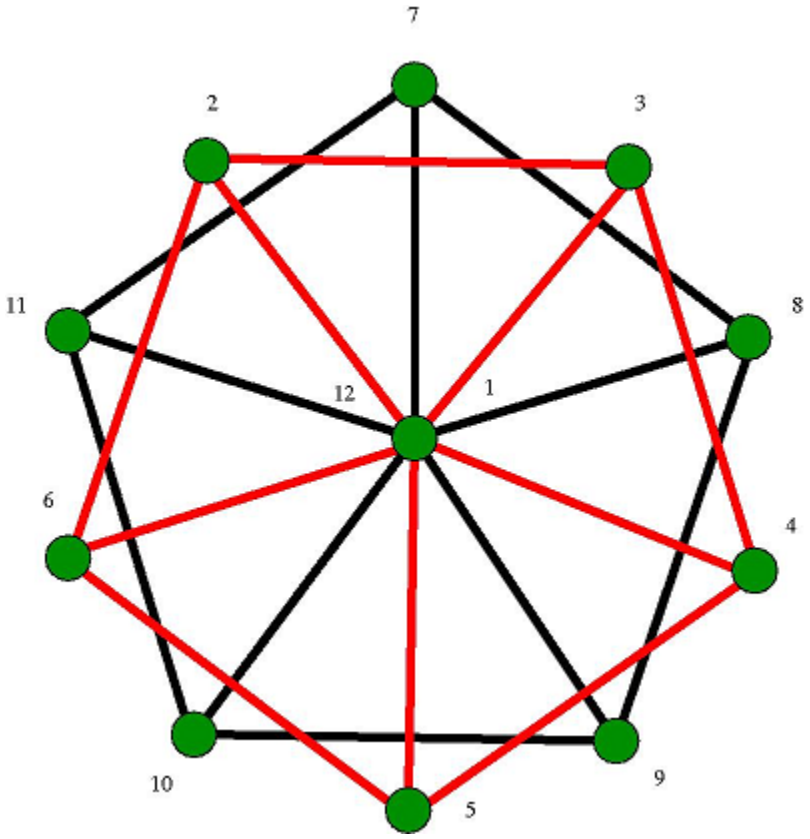

Figure 5. The Arrangement of the vertices on an Icosahedron.

The apical point has the position *[0,0,R]*. For the surrounding points, the azimuthal angle between adjacent vertices is given by

$$\Phi_I = \frac{2\pi}{5} = 72^o$$

It is important to note here that this angle is only the difference between the angles azimuthally, and it is not the full angle between the vectors drawn from the icosahedrons center to the corresponding vertices. We will need to be very careful in calculating this angle which we denote by "θ_I".

The coordinates of the upper hemisphere are thus:

$$\boldsymbol{V_1}: (Apex) \quad R[0,0,1]$$

$$\boldsymbol{V_2}: R[\sin\theta_I, 0, \cos\theta_I]$$

$$\boldsymbol{V_3}: R[\sin\theta_I \cos(\Phi_I), \sin\theta_I \sin(\Phi_I), \cos\theta_I]$$

$$\boldsymbol{V_4}: R[\sin\theta_I \cos(2\Phi_I), \sin\theta_I \sin(2\Phi_I), \cos\theta_I]$$

$$\boldsymbol{V_5}: R[\sin\theta_I \cos(3\Phi_I), \sin\theta_I \sin(3\Phi_I), \cos\theta_I]$$

$$\boldsymbol{V_6}: R[\sin\theta_I \cos(4\Phi_I), \sin\theta_I \sin(4\Phi_I), \cos\theta_I]$$

Looking at the lower hemisphere, we notice that the Nadir (point 12) is surrounded by five points where the angular separation from the Nadir is θ_I, in each case as may be seen through symmetry arguments. Again, appealing to the icosahedral symmetry, we see that the adjacent points differ by exactly the same $\Phi_I = \frac{2\pi}{5}$ relationship we used in the upper hemisphere. However, it is important to note that the vertex 7 is offset from its upper hemisphere counterpart vertex 2 by the angle $\frac{\Phi_I}{2}$. So now we have for the vertex positions:

$$\boldsymbol{V_7}: R[\cos(\frac{\Phi_I}{2})\sin\theta_I, \sin(\frac{\Phi_I}{2})\sin\theta_I, -\cos\theta_I]$$

$$\boldsymbol{V_8}: R[\cos(\frac{3\Phi_I}{2})\sin\theta_I, \sin(\frac{3\Phi_I}{2})\sin\theta_I, -\cos\theta_I]$$

$$\boldsymbol{V_9}: R[\cos(\frac{5\Phi_I}{2})\sin\theta_I, \sin(\frac{5\Phi_I}{2})\sin\theta_I, -\cos\theta_I]$$

$$\boldsymbol{V_{10}}: R[\cos(\frac{7\Phi_I}{2})\sin\theta_I, \sin(\frac{7\Phi_I}{2})\sin\theta_I, -\cos\theta_I]$$

$$\boldsymbol{V_{11}}: R[\cos(\frac{9\Phi_I}{2})\sin\theta_I, \sin(\frac{9\Phi_I}{2})\sin\theta_I, -\cos\theta_I]$$

$$\boldsymbol{V_{12}}: (Nadir)\ \ R[0,0-1]$$

Now we have the task of calculating the angle θ_I. We will do so by referring to figure 5, and noting that the nearest neighbors of site 1 are {2,3,4,5,6}. On the other hand sites 2 and 3 are also mutual nearest neighbors. By equating the dot products between the vectors associated with vertices 1 and 2 and between 2 and 3 we can determine this angle. So:

$$\boldsymbol{V_1}.\boldsymbol{V_2} = \boldsymbol{V_2}.\boldsymbol{V_3}$$

$$R^2[\cos\theta_I] = R^2[(\cos\theta_I)^2 + \cos\Phi_I\,(\sin\theta_I)^2]$$

This, with some algebra gives

$$\cos\theta_I = (\cos\theta_I)^2\,(1-\cos\Phi_I) + \cos\Phi_I$$

$$\cos\theta_I = \frac{1}{2-2\cos\Phi_I}[1 \pm (1-2\cos\Phi_I)]$$

If we take the positive root, then we simply obtain unity for $\cos\theta_I$, so we must take the negative root. Therefore we finally have:

$$\cos\theta_I = \frac{\cos\Phi_I}{1-\cos\Phi_I} = \frac{\cos(\frac{2\pi}{5})}{1-\cos(\frac{2\pi}{5})}$$

With the above relationship, we can now determine the length of the edge of an icosahedron in terms of the radius R of the circumscribing sphere. The distance between points 1 and 2 is given by

$$S = \|\boldsymbol{V_1} - \boldsymbol{V_2}\|$$

But

$$S^2 = \boldsymbol{V_1^2} + \boldsymbol{V_2^2} - 2\boldsymbol{V_1}\boldsymbol{V_2} = 2R^2 - 2R^2\boldsymbol{V_1}\boldsymbol{V_2} = 2R^2[1 - \cos\theta_I]$$

And with the expression found for $\cos\theta_I$ we find that:

$$S = 1.0515R$$

$$R = 0.95106S$$

This means that the edge length and the radius of the sphere are nearly the same. Now we are ready to tackle the full three dimensional problem.

We will follow the assumption that the charge-carriers move very rapidly among the sites on the same Icosahedron and the jumps from one Icosahedron to another is much less frequent. We shall center an s-orbital on each vertex of the Icosahedron. As such we will take $r = \frac{S}{2}$ or $R \approx 2r$ which leads to realm of the influence of each icosahedron extending another half radius beyond the circumscribing sphere. Now we place each icosahedron on the points of a three dimensional tetrahedral lattice. The task is now to calculate the overlap integral among two neighboring icosahedra as a function of the distance between them.

The Overlap Integrals of Neighboring Icosahedra

Consider two icosahedra separated by a distance *d*. we will designate one "cage" by *i,* and the other by the label *j.* The wave function on the icosahedron labeled *i* will be represented by the summation:

$$\Psi_i^{Total} = \sum_{k=1}^{12} \psi_i^k$$

Following a similar convention to denote the wave function for the *j* cage, we can now define the product and consequently the overlap integral as:

$$\Psi_j^{total}\Psi_i^{total} = \sum_{k'=1}^{12}\sum_{k=1}^{12} \psi_j^{k'}\,\psi_i^k$$

$$I_{ij} = \sum_{k=1}^{12}\sum_{k'=1}^{12}\iiint_{-\infty}^{\infty} \psi_i^k \psi_i^{k'} dxdydz$$

We can see that many individual terms of the overlap integral will depend only on the distance $d_{ik\text{-}jk'}$ separating the vertices of the icosahedrons. To find this distance, first let us examine the case where there is no difference in the orientation among the two icosahedra, although there is a separation of distance *d* between them. Then:

$$d_{ik-jk'} = \left|\boldsymbol{r}_{ik} - \boldsymbol{r}_{jk'}\right|$$

So that

$$d_{ik-jk'} = |\boldsymbol{V}_k - \boldsymbol{d} - \boldsymbol{V}_{k'}|$$

Then we have

$$d_{ik-jk\prime}^2 = (V_k)^2 - 2\boldsymbol{V}_k(\boldsymbol{d} + \boldsymbol{V}_{k'}) + (\boldsymbol{d} - \boldsymbol{V}_k)^2$$

$$= (V_k)^2 - 2\boldsymbol{V}_{k\prime}\boldsymbol{d} - 2\boldsymbol{V}_k\boldsymbol{V}_{k\prime} + d^2 - 2\boldsymbol{V}_k\boldsymbol{d} + (V_k)^2$$

We note here that $R^2 = V_k^2 = V_{k\prime}^2$ we see that we have finally:

$$d_{ik-jk\prime} = \sqrt{d^2 + 2R^2 - 2d(\boldsymbol{V}_k + \boldsymbol{V}_{k\prime}) - 2\boldsymbol{V}_k\boldsymbol{V}_{k\prime}}$$

As such we can calculate these quantities which are easily handled by a computer. Now we wish to calculate integrals of the form:

$$\iiint_{-\infty}^{\infty} \psi_i(x,y,z)\psi_j(x,y,z)dxdydz$$

For this purpose we use $\psi_i = e^{-\alpha r_i}$ and $\psi_j = e^{-\alpha r_j}$ where r_i and r_j are the respective distances of a point in space. We can make use of the inherent azimuthal symmetry of the problem. If we assume that the points *i* and *j* are along the z-axis, then we have:

$$r_i = \sqrt{x^2 + y^2 + (z - \frac{d}{2})^2}$$

$$r_j = \sqrt{x^2 + y^2 + (z + \frac{d}{2})^2}$$

And now, substituting back into the above integral we have a unique situation in which the integrand is constant (and attains its highest value) along the line connecting nuclei *i* and *j*. In the case that $x = y = 0$ we have $r_i + r_j = d$. Now let us operate in the cylindrical coordinates and graph the contours of constant values in the integrand. We

seek curves with the requirement that $r_i + r_j = r + \epsilon$ where $\frac{\epsilon}{2}$ is the difference between the semi-major axis and $\frac{d}{2}$. This condition, that $r_i + r_j = d + \epsilon$, is necessary and sufficient to define and ellipse in the ρ-z plane. This ellipse, when rotated about the z-axis is an ellipsoid, a prolate three dimensional figure with a major axis of length *2a* and two minor axes each of length *2b.* The volume of this ellipsoid is

$$V = \frac{4\pi}{3}(ab^2) = \frac{4\pi ab^2}{3}$$

We need to calculate the quantities *a* and *b*. in the ρ-z plane, the cross section of the prolate ellipsoid is a standard ellipse with semi-major axis *a* and the semi-minor axis *b.* to start the calculation, we begin with the condition $r_i + r_j = d + \epsilon$ and noting the definitions for r_i and r_j we square both sides of our condition and therefore:

$$r_i^2 + r_j^2 + 2r_i r_j = (\epsilon + d)^2$$

For later convenience we do not expand the right side immediately. However, we should isolate the $2r_ir_j$ term and then square both sides again to remove the remaining radicals. This leads to:

$$(2r_i r_j)^2 = \{(\epsilon + d)^2 - r_i^2 - r_j^2\}$$

$$0 = (\epsilon + d)^4 - 2[r_i^2 + r_j^2](\epsilon + d)^2 + r_i^4 - 2r_i^2 r_j^2 + r_j^4$$

Substituting for the *r*'s and with a bit of algebra, we arrive at:

$$(\epsilon + d)^2[(\epsilon + d)^2 - d^2] = 4\rho^2(\epsilon + d)^2 + 4z^2[(\epsilon + d)^2 - d^2]$$

Diving both sides by $(\epsilon + d)^2[(\epsilon + d)^2 - d^2]$ leads to:

$$1 = \frac{4\rho^2}{[\epsilon^2 + 2d\epsilon]} + \frac{4z^2}{(\epsilon + d)^2}$$

So we see that $a = \frac{1}{2}(\epsilon + d)$ and $= \frac{1}{2}(\varepsilon^2 + 2\epsilon d)^{\frac{1}{2}}$. Therefore the volume of the prolate ellipsoid is given by:

$$V = \frac{\pi}{6}[\epsilon^3 + 3d\epsilon^2 + 2\epsilon d^2]$$

Now our interest is in the differential volume shift δV which accompanies an infinitesimal variation δc in the parameter controlling the shape of the ellipse. We may calculate:

$$\delta V = \frac{\partial V}{\partial \epsilon}\delta\epsilon = \pi\left[\frac{1}{2}\epsilon^2 + d\epsilon + \frac{1}{3}d^2\right]\delta\epsilon$$

The contribution of the integral form of this shell of the ellipsoid will be given by the expression:

$$I_j^i = \int_0^\infty e^{-\alpha[d+\epsilon]}\delta V = \pi e^{-\alpha d}\int_0^\infty \left[\frac{1}{2}\epsilon^2 + d\epsilon + \frac{1}{3}d^2\right]e^{-\alpha\epsilon}\delta\epsilon$$

This yields

$$I_j^i = \frac{\pi}{\alpha}e^{-\alpha d}[\alpha^{-2} + \frac{d}{\alpha} + \frac{d^2}{3}]$$

The above result is the full overlap integral between the sites *i* and *j*. This result has been carefully checked using numerical Monte Carlo integration, finding agreement up to a part within 100,000 or so. We shall use this result to calculate the overlap between Icosahedral B_4C cages.

The Rotations of the Icosahedra

Finally, we must introduce a random shift in the orientation of the Icosahedra. To do this, we consider a set of vectors centered at the origin. We wish to rotate this system by an angle θ about an axis which we will label $\mathbf{V}_o$. We may break up the rotating vectors in two components: a parallel component which will not change through this rotation and a perpendicular component which will experience the rotation about $\mathbf{V}_o$. now we wish to define for each vector a set or orthogonal axes so that:

$$\boldsymbol{V}_i = V_i^{\parallel}\hat{V}_o + V_i^{\perp}\widehat{V_i^{\perp}}$$

Now we need a 3rd vector which will be perpendicular to both $\hat{V}_o$ and $\widehat{V_i^{\perp}}$. We can find this vector using the cross product; however we first must define $V_i^{\perp}$ explicitly. Here, we can use the dot product to calculate the component of $\mathbf{V}_i$ parallel to $\mathbf{V}_o$ and subtract this piece from $\mathbf{V}_i$. if we normalize this vector, then we would have the sought after component. This leads to:

$$V_i^{\perp} = \frac{[V_i - \hat{V}_o(\boldsymbol{V}_i.\hat{V}_o)]}{\|V_i - \hat{V}_o(\boldsymbol{V}_i.\hat{V}_o)\|}$$

Now let us consider that $\mathbf{V}_o$ to be the $\hat{z}$ unit vector and the $V_i^{\perp}$ is the $\hat{x}$ unit vector. Then using the right hand rule to produce the correct $\hat{y}$ vector we have $\hat{V}_o \; X \; \widehat{V_i^{\perp}}$. Finally, the rotation which occurs in the $\widehat{V_i^{\perp}}$- $(\hat{V}_o \; X \; \widehat{V_i^{\perp}})$ plane by the angle θ produces a new vector given by:

$$\boldsymbol{V}_i' = [\,\|\boldsymbol{V}_i^{\parallel}\|\hat{V}_o + \|\widehat{V_i^{\perp}}\|\cos(\theta)\widehat{V_i^{\perp}} + \|\widehat{V_i^{\perp}}\|\sin(\theta)\widehat{V_i^{\perp}}$$

Using this method we can determine the new vectors under any rotations about a certain axis with a certain angle. This method is very easy, and can be very simply implemented within a program.

CHAPTER 3

RESULTS AND DISCUSSION

Implementation of the Program

Armed with the information in the previous chapter, we are now ready to proceed with implementing our code, for which we used the FORTRAN programming language as it is the language that the authors are most familiar with. The ultimate goal of this program is to be self consistent. That is to say, we would start with very few assumptions, and implement them in the most basic situation. We will then study the behavior of the results of this simple case, and successively apply it to more complex cases, and so on. To this end, we will start by looking at the 2-dimensional code first (the results of the 1-dimensional case are trivial, and do not shed much light at the situation).

The Determination of an Acceptable Size of the System

The first task is to determine the size of the system. The importance of this step is twofold; first, due to the periodic boundary conditions we employ, we need to make sure that the system is large enough such that the condition for the material to be amorphous is met (i.e. the lack of long range order in the structure). Second, due to the nature of the complex calculations in the program, we would like the system to be as small as possible to meet the first condition, yet not too large as to make the calculations extremely time consuming.

To this end, we looked at the convergence of the residual fluxes, which is the measure for the error in our system, for various system sizes, which we present in Graph 1.

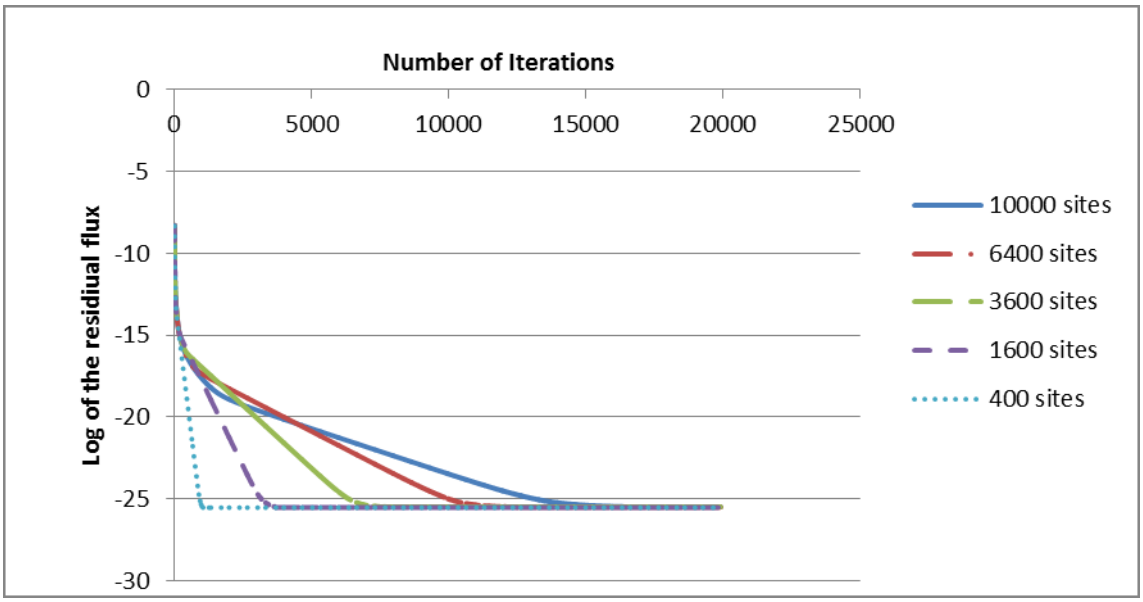

Graph1. The convergence of the residual flux for 2-D systems of various sizes.

As expected, as the number of sites increases, so too does the number of iterations required to achieve conservation of current. The important implication here is that our code achieves this conservation of current for all systems ranging from 20X20 and up to 100X100. Therefore we need not consider very large systems for the 3-dimentional case. Instead, we opt to test this condition for systems which range from

10X10X10 and up to 40X40X40 in the 3-dimensional case, the results of which are presented in Graph 2.

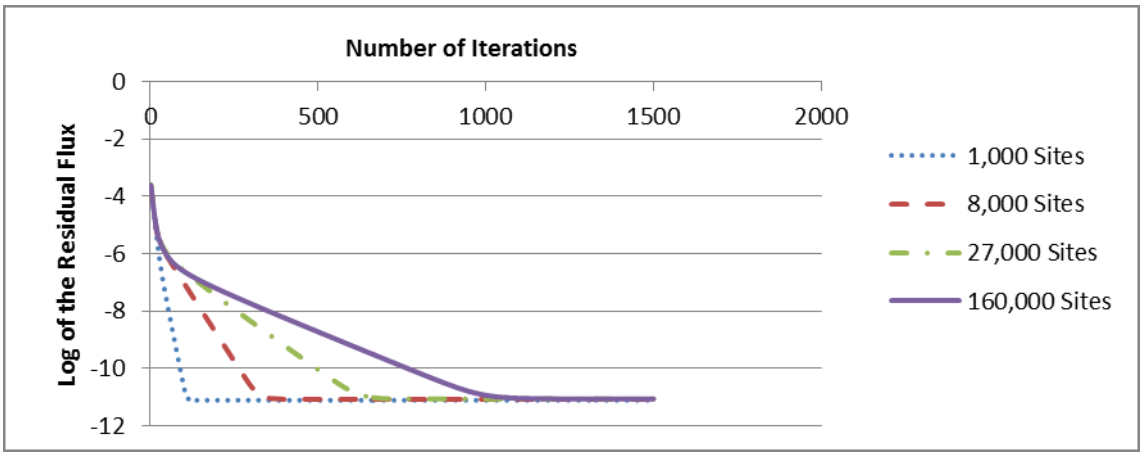

Graph 2. The convergence of the residual flux for 3-D systems of various sizes

It is worth mentioning that the convergence in the 3-dimensional case happens faster, and sooner. This is due to the fact that our program loses some accuracy with the addition of the 3rd dimension. Nevertheless, the residual flux converges at 10^{-12} which is to a good approximation equal to zero.

The Effects of the Electric Field

For our study, we would like to see how the electric field would affect the flux of charge carriers at each point. To do this, we must find the steady state flux where no field is applied, and subtract this from the total flux in the presence of an electric field. Thus we can isolate the behavior of our system due to the electric field only. In Figure 6

we first have a snapshot of the jumps, or the net flux, at each point without the presence of the electric field:

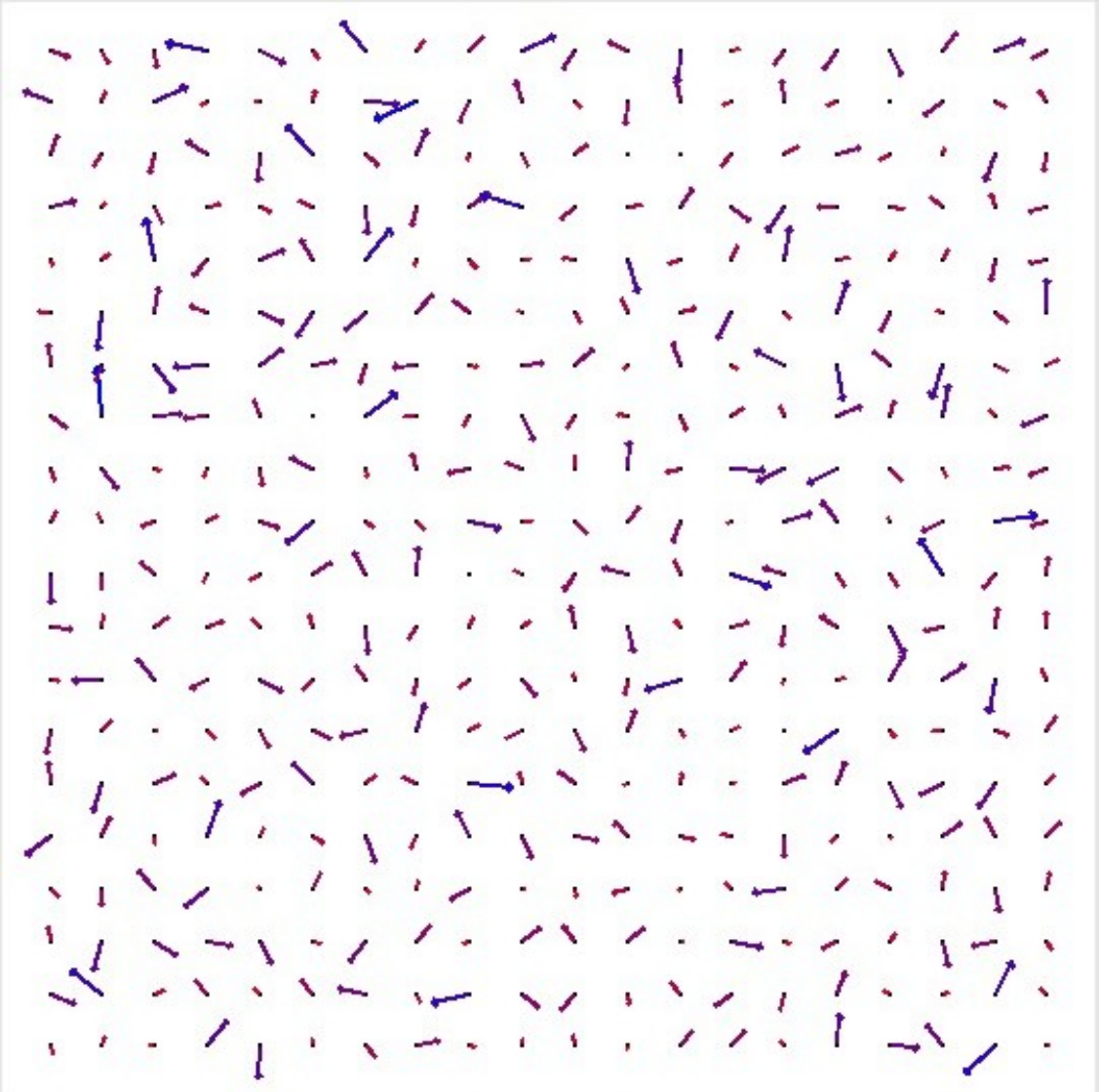

Figure 6. The Net flux at each site without the presence of an electric field.

Now, we subtract this result from the total net flux in the presence of an electric field. The result is shown in Figure 7.

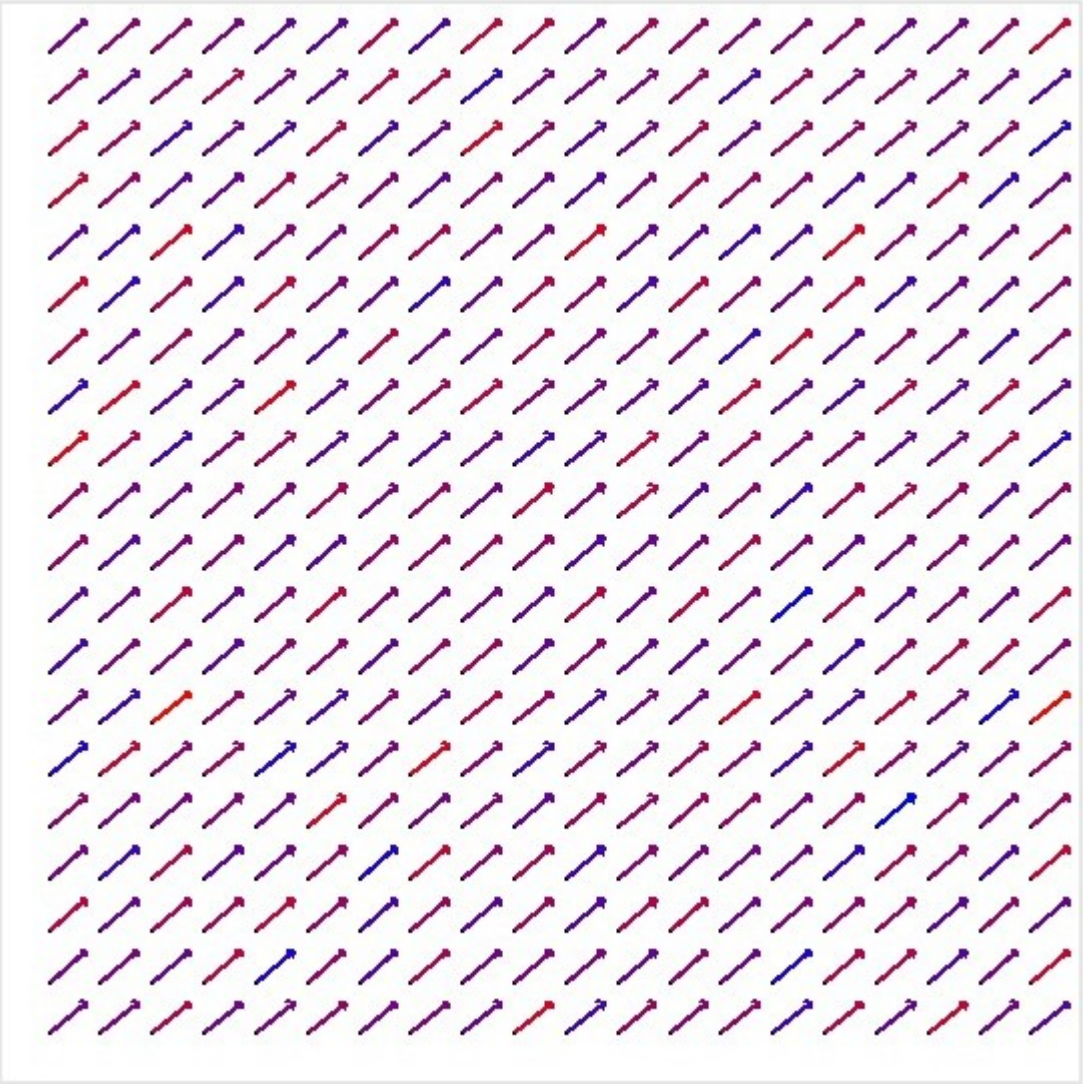

Figure 7. The net flux due to the electric field minus the flux of the steady state case.

This is the flux-vector due purely to the electric field. The very nearly parallel orientation of the flux-vectors is strikingly evident in the graph, and we are now able to address the problem of only considering the nearest neighbor when considering the hops of each site.

Consideration of the Nearest Neighbors

For the purpose of the determination of the effects of considering varying nearest neighbors, we suppress the perturbations to the orientation and to the radii of the icosahedrons. Thus we look at the effect of the change in the flux at each site due to perturbations to the lattice constant in while considering jumps to only the nearest neighbor, and then up to the second nearest neighbor, and so on.

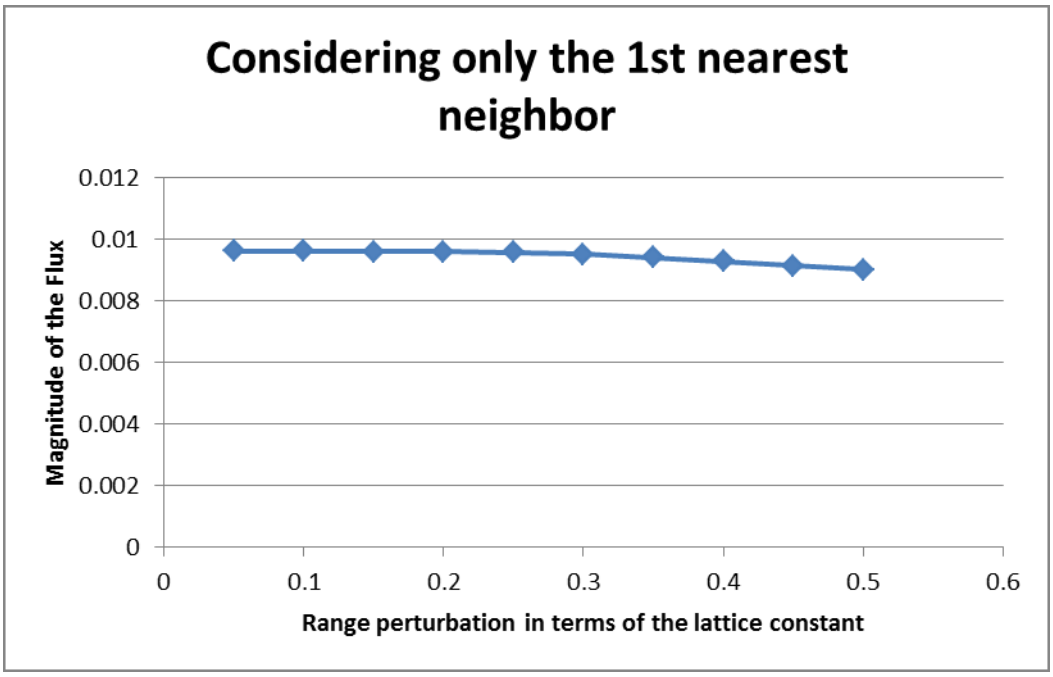

Graph 3. Perturbing the range while considering only the 1st nearest neighbor.

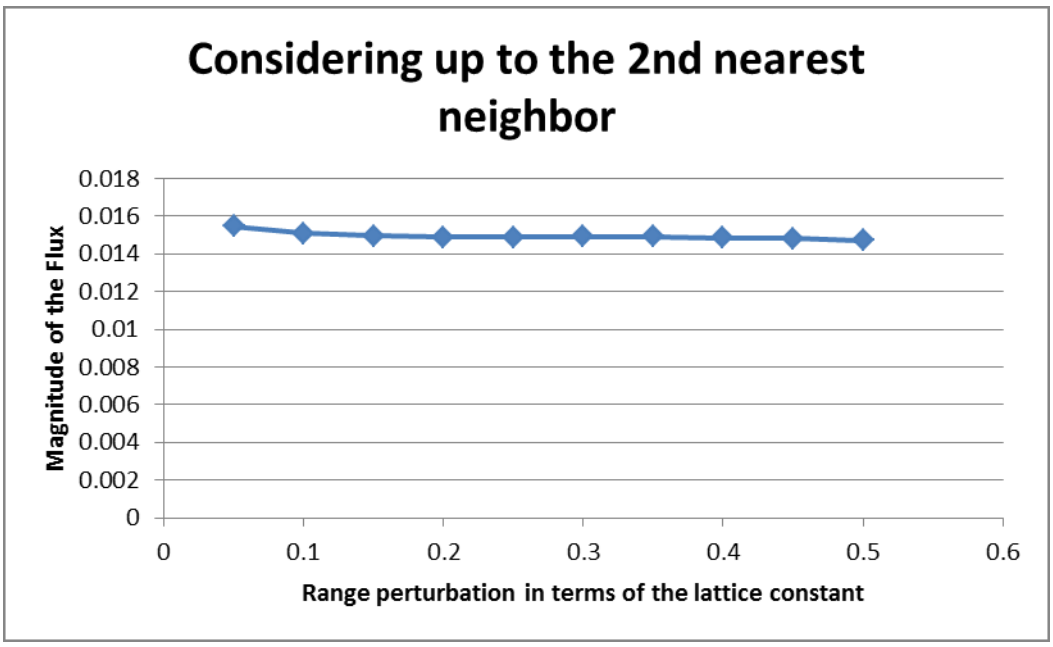

Graph 4. Perturbing the range while considering up to the 2nd nearest neighbor.

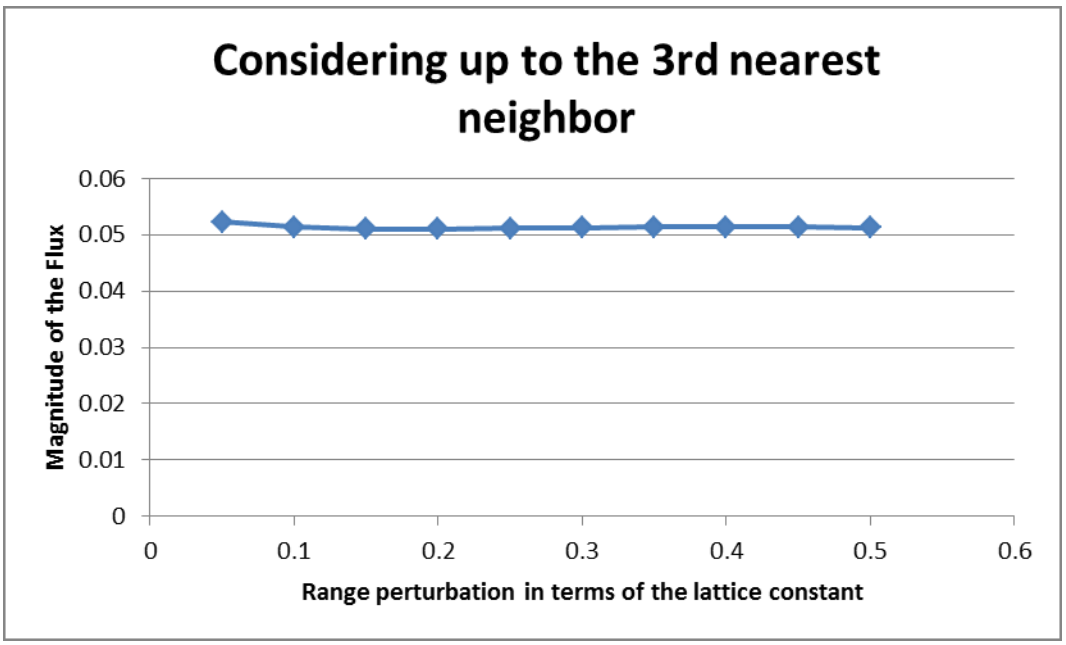

Graph 5. Perturbing the range while considering up to the 3rd nearest neighbor.

From the above graphs we can see that increasing the number of nearest neighbors has a noticeable effect on the magnitude of the flux, which is to be expected. Another facet of increasing the number of nearest neighbors is that it decreases the sensitivity to perturbing the lattice constant.

Finally, we need to check the statistical integrity of our program. The code we used utilizes a random number generator called Mersenne twister, which has been regarded for a very long time as the best pseudo-random number generator (PRNG) available. This PRNG uses a seed value allocated by the user, and generates a sequence of random numbers which are the same for a given seed. This allows us to test for the statistical integrity of our code by running the same version of the code with different seeds.

For this, we have chosen to suppress the variations in the radii and the lattice perturbations, and only perturb the orientation of the Icosahedra.

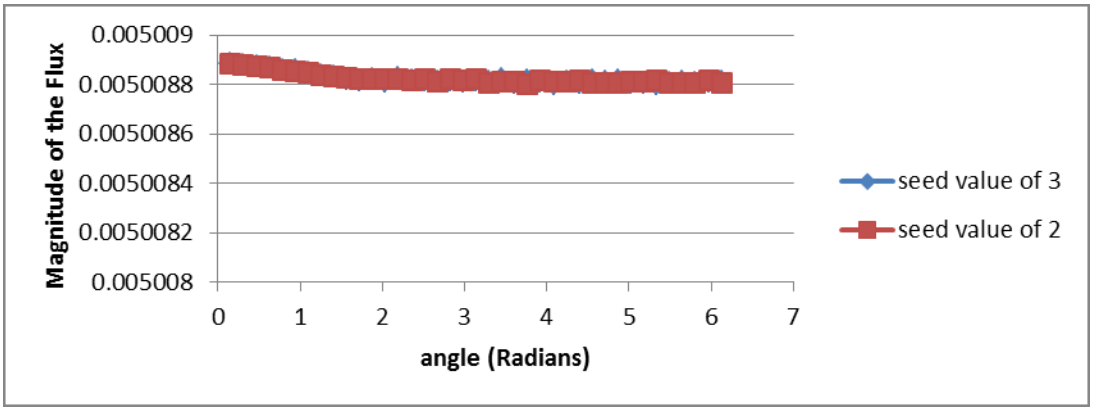

Graph 6. The test of different seed values for the PRNG.

As seen in graph 6, the behavior of our system is independent of the seed value allocated. We are now ready to run the code while considering perturbations to the orientation, the radii, and the lattice constant simultaneously.

Results of the Full Icosahedral Code

For this part, we used a system size of 30^3 sites, with the decay constant set to be equal to 1 lattice constant. Due to the extremely long time required to run this code, we opted to consider only the first nearest neighbor, and examine the behavior of our system. This constraint can be relaxed given a more powerful computing device, or when parallel computing is accessible. The perturbations to the lattice constant and the radii ranged from 0 to 0.5a, and the orientations were perturbed by a range from 0 to π.

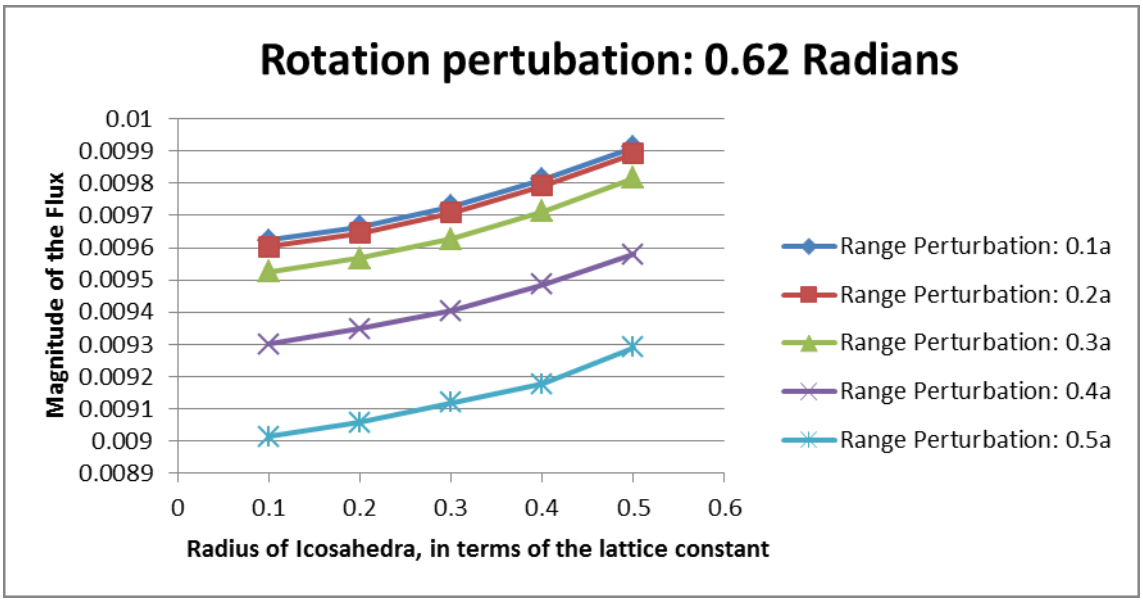

Graph 7. Perturbations to the lattice constant and the radius at 0.62rad orientation shift.

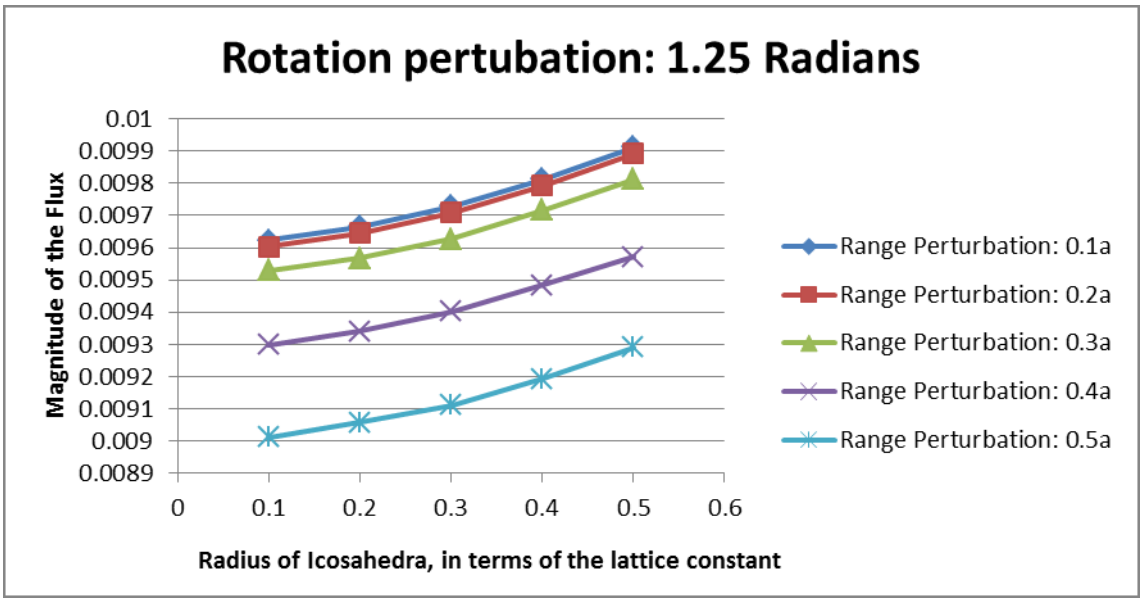

Graph 8. Perturbations to the lattice constant and the radius at 1.25rad orientation shift.

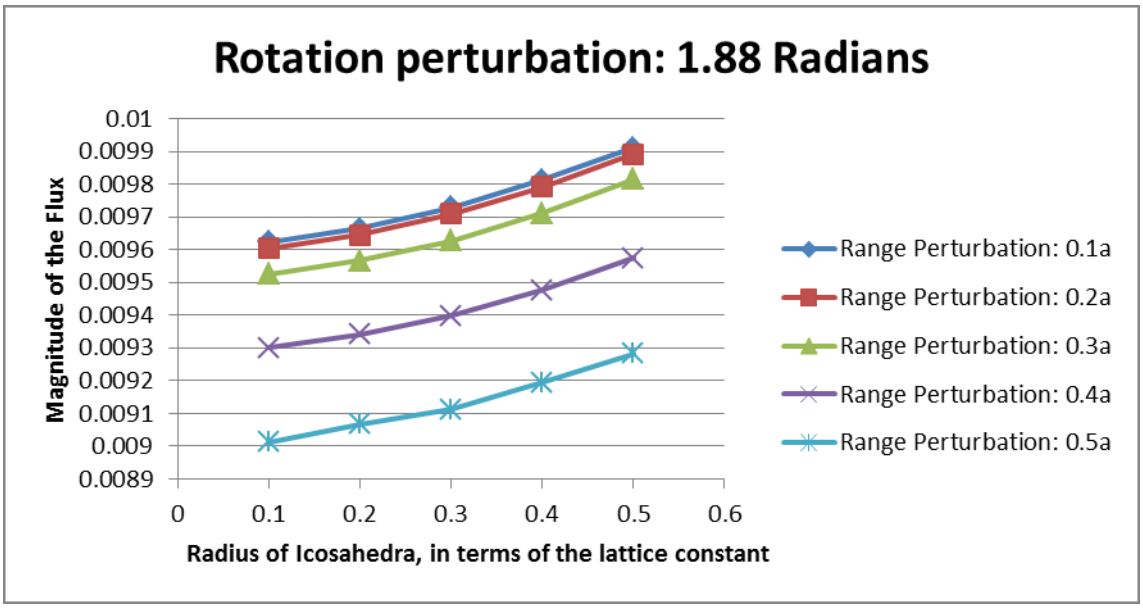

Graph 9. Perturbations to the lattice constant and the radius at 1.88rad orientation shift.

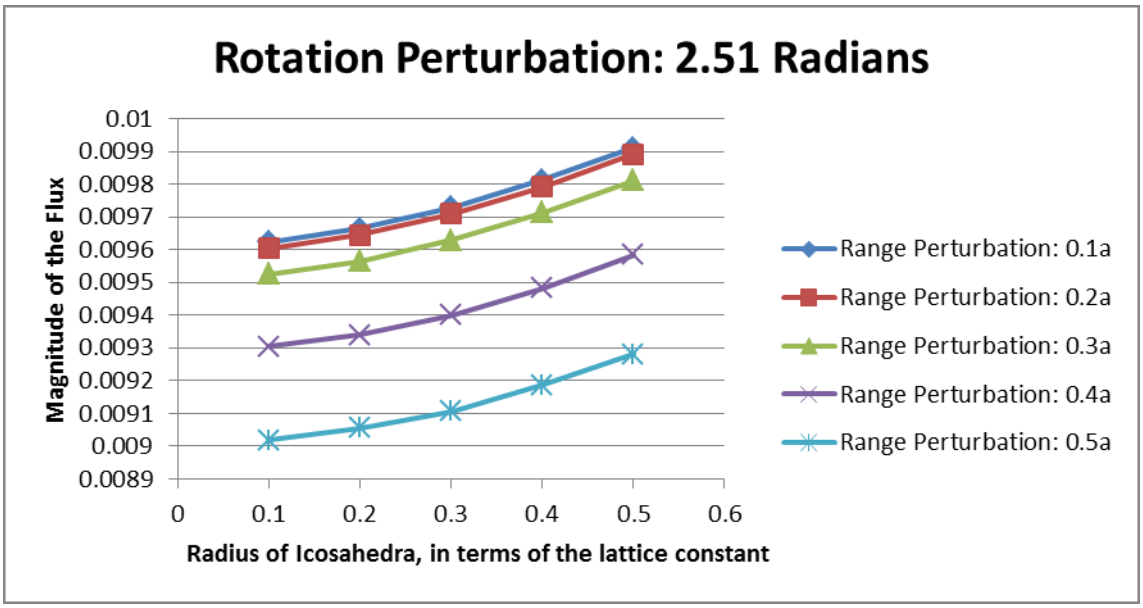

Graph 10. Perturbations to the lattice constant and the radius at 2.51rad orientation shift.

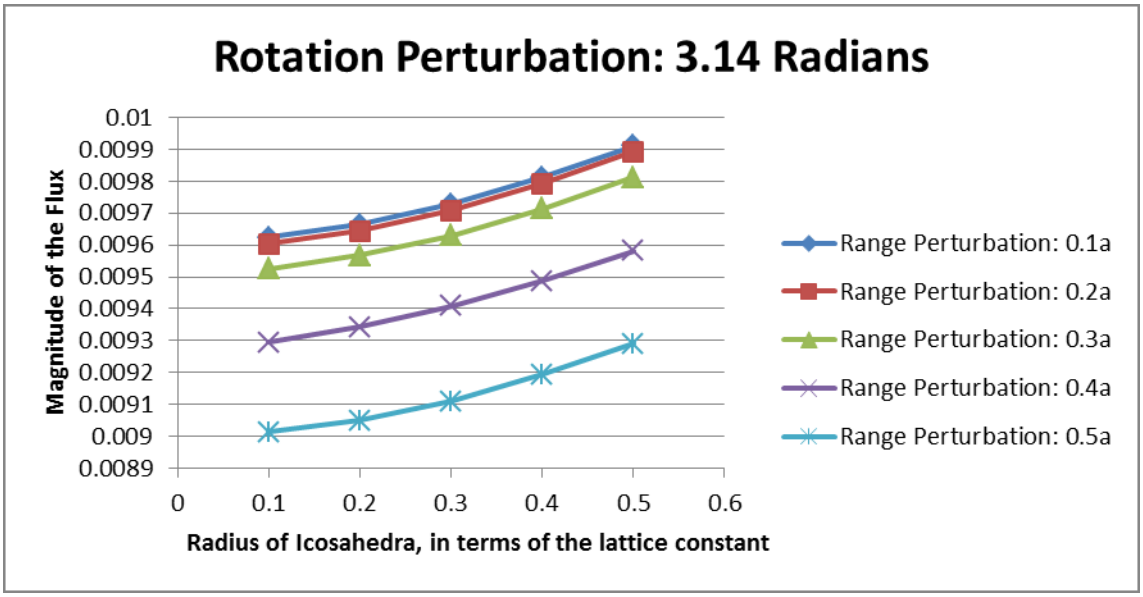

Graph 11. Perturbations to the lattice constant and the radius at 3.14rad orientation shift.

From the previous graphs it is immediately apparent that the perturbations to the orientation have no effect on the magnitude of the flux. This result allows us to eliminate the perturbations to the orientation, and our task becomes that of varying two variables: the range and the radius. For this we have used the exact same system while suppressing the perturbation to the orientation.

First, we vary the radii of the icosahedrons for a given range, given in graph 12, and then we did the reverse, i.e. varying the range perturbation for a given radius, in graph 13.

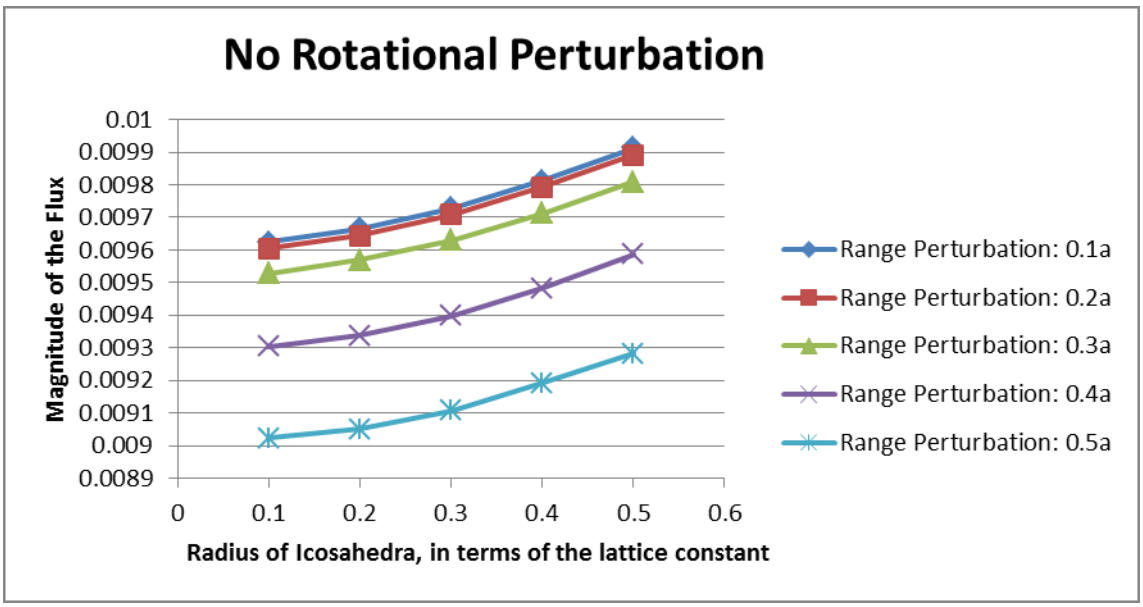

Graph 12. Varying the radii for a given perturbation to the lattice constant.

From graph 12 we can see that the increase in the radius corresponds to an increase in the magnitude of the flux. This is due to the fact that larger Icosahedra are closer together, and therefore the possibility of a jump between two neighboring icosahedra increases proportionally.

Furthermore, this effect is more pronounced with larger perturbations to the lattice constant. This is due to the greater possibility of larger icosahedra to intrude into the critical radius within which the hops are more probable.

Now we turn our attention to the reverse case, shown in graph 13.

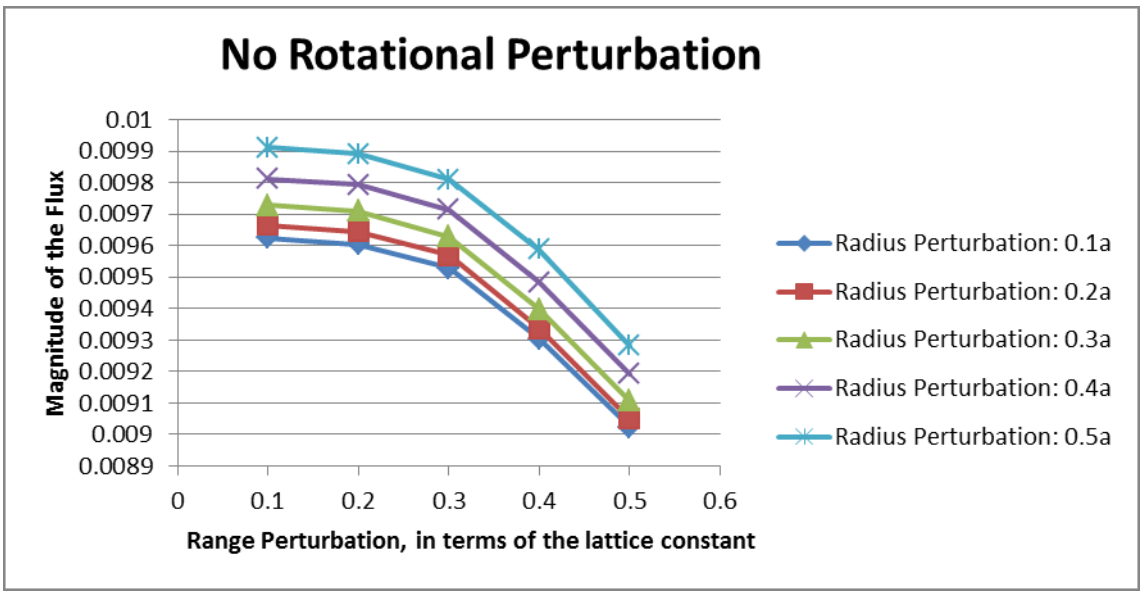

Graph 13. Varying the perturbation to the lattice constant given a radius.

The effects of the range follow the same pattern for each specified radius, although each value of the radius shifts the magnitude of the flux up, due to the larger possibility of a hop to occur with the larger icosahedra.

From the comparison of graphs 12 and 13 it is apparent that the jumps between the icosahedral cages are determined by the smallest distance between the vertices of neighboring icosahedra. This essentially combines the perturbations to the range and the radii into a single parameter which determines the conductivity behavior within this system.

CHAPTER 4

CONCLUSION

Summary

From the above work, we believe that we have correctly developed a numerical method with which to tackle the issue of conductivity in amorphous materials. We have applied this method to a specific system, a random collection of Icosahedral cages, and determined that to a large extent, the conductivity is mostly dependent on the spatial distance between the Icosahedral vertices of neighboring sites and is completely independent of the perturbations to the orientations of the cages. We find weak sensitivity (a slight decrease in the charge flux magnitude on the order of a few percent) to the translational disorder, in which the positions of the icosahedral clusters are perturbed. Hence, transport characteristics appear to be largely robust with respect to disorder in the context of our iso-energetic variable range hopping treatment.

Future Works

In the future, we wish to relax one more assumption inherent in our study above; which is the Iso-energetic assumption. That is, to consider a system where the energy of the sites vary by an integer multiple of kT.

Furthermore, we would also like to consider the effects of the Coulomb force on the hops. We suspect that this effect will play a larger role in highly populated systems, and may drastically change the analysis.

Finally, as noted previously we believe that a simple analytical solution for this system exists. We wish to derive it with the full consideration of the Coulomb force.

BIBLIOGRAPHY

[1] Mott, N.F., *Phil. Mag*., **19** (1969) 835.

[2] Apsley, N. and Hughes, H.P., *Phil. Mag*., **30** (1974) 963.

[3] Miller, A. and Abrahams E., *phys. Rev*. **120** (1960) 745.

[4] Marshall, J.M. and Main C., *J. Physics: Condensed Matter* **20** (2008) 285210.

[5] Mott, N.F. and Davis, E.A., *Electronic Processes in Non-Crystalline Materials*, 2nd Ed. Clarendon Press, Oxford (1979).

[6] Marshall, J.M. and Arkhipov, V.I., *J. optoelectron. Adv. Mater.* **7** (2005) 43.

[7] Paul, D.K. and Mitra, S.S., *Phys. Rev. Lett.,* **31** (1973) 1000.

[8] Lindemann, F.R., Z. Phys. **11**, (1910) 609.

VITA

Naseer A. Dari was born on July 22, 1983 in Baghdad, Iraq. In 1999 he immigrated to the United States alongside his family, where he attended northeast high school in Kansas City, Missouri. In 2008 he graduated with a B.S. in physics from University of Missouri-Kansas City, and enrolled in the graduate school to earn his Masters in Physics.